Available online at www.sciencedirect.com
ScienceDirect
Applied Geochemistry 22 (2007) 2834–2860
Applied Geochemistry
www.elsevier.com/locate/apgeochem

Hydrochemical and isotopic tracing of mixing dynamics and water quality evolution under pumping conditions in the mine shaft of the abandoned Frances Colliery, Scotland

Trevor Elliot [a,*], Paul L. Younger [b]

[a] EERC Environmental Tracers Laboratory (ETL), Environmental Engineering Research Centre, School of Planning, Architecture and Civil Engineering, Queen's University Belfast, BT9 5AG Northern Ireland, UK
[b] Hydrogeochemical Engineering Research and Outreach (HERO), Institute for Research on the Environment and Sustainability (IRES), University of Newcastle Upon Tyne, Newcastle Upon Tyne NE1 7RU, UK

Received 13 September 2006; accepted 1 July 2007
Editorial handling by P.B. McMahon
Available online 15 August 2007

Abstract

Since 1995, when pumps were withdrawn from deep mines in East Fife (Scotland), mine waters have been rebounding throughout the coalfield. Recently, it has become necessary to pump and treat these waters to prevent their uncontrolled emergence at the surface. However, even relatively shallow pumping to surface treatment lagoons of the initially chemically-stratified mine water from a shaft in the coastal Frances Colliery during two dynamic step-drawdown tests to establish the hydraulic characteristics of the system resulted in rapid breakdown of the stratification within 24 h and a poor pumped water quality with high dissolved Fe loading. Further, data are presented here of hydrochemical and isotopic sampling of the extended pump testing lasting up to several weeks. The use in particular of the environmental isotopes $\delta^{18}O$, $\delta^{2}H$, $\delta^{34}S$, ^{3}H, ^{13}C and ^{14}C alongside hydrochemical and hydraulic pump test data allowed characterisation of the Frances system dynamics, mixing patterns and water quality sources feeding into this mineshaft under continuously pumped conditions. The pumped water quality reflects three significant components of mixing: shallow freshwater, seawater, and leakage from the surface treatment lagoons. In spite of the early impact of recirculating lagoon waters on the hydrochemistries, the highest Fe loadings in the longer-term pumped waters are identified with a mixed freshwater–seawater component affected by pyrite oxidation/melanterite dissolution in the subsurface system.

1. Introduction

Water quality stratification in flooded underground coal workings following mine abandonment and cessation of pumping has been recognised sporadically in the literature, but only recently are the implications for the planning and operation of pollution prevention/remediation measures being assessed.

The coastal Frances Colliery (UK National Grid Reference: NT 310 938) is part of the East Fife or Dysart Leven Coalfield in Fife, Scotland (Fig. 1).

* Corresponding author. Tel.: +44 28 90974736; fax: +44 28 90663754.
E-mail addresses: t.elliot@qub.ac.uk (T. Elliot), paul.younger@ncl.ac.uk (P.L. Younger).

0883-2927/$ - see front matter © 2007 Elsevier Ltd. All rights reserved.
doi:10.1016/j.apgeochem.2007.07.007

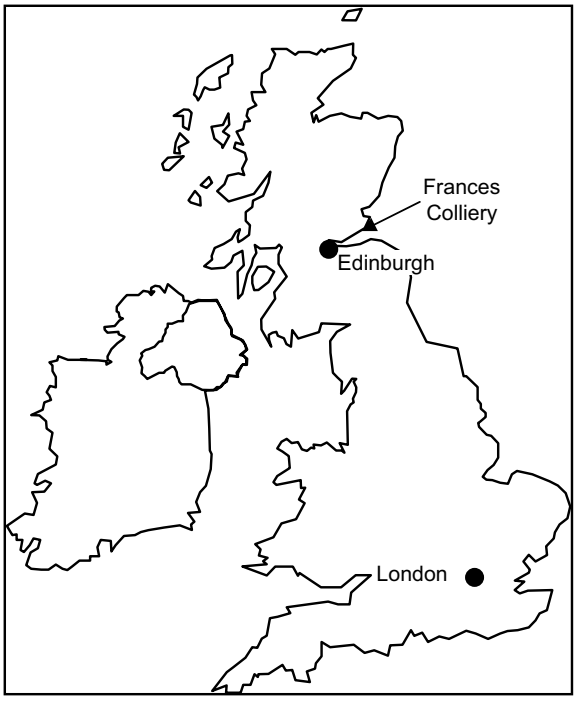

Fig. 1. Map showing the UK location of the Frances Colliery (National Grid Reference: NT 310 938) in the East Fife or Dysart Leven Coalfield, Fife, Scotland.

The coalfield comprises Coal Measures strata of Westphalian (Carboniferous) age that were subjected to folding during the Late Carboniferous. The Frances Colliery with subsurface workings both onshore and extending offshore lies near the trough of a syncline in which a c. 500 m thick Coal Measures cyclothermic sequence of alternating sandstone, limestone and shale beds is preserved with around 20 coal seams (Fig. 2). A chronology of the major operational events relevant to the Frances Colliery is given in Table 1. During active colliery operations (i.e. prior to closure and abandonment), dewatering of the mineworkings necessarily exposed chemically-reduced sulfides associated especially with the high-S content coal seams in marine bands (e.g., the monosulfide, FeS, and also pyrite, FeS_2) to the ingress of O_2 in air over a period of decades. This would (e.g. Douglas and Beveridge, 1998; Kendelewicz et al., 2004; Gasharova et al., 2005) give rise to a veneer of oxidised products typically including efflorescent minerals such as: Melanterite [$FeSO_4 \cdot 7H_2O$], Rozenite [$FeSO_4 \cdot 4H_2O$], Szomolnokite [$FeSO_4 \cdot 4H_2O$], Copiapite [$Fe^{2+}(Fe^{3+})_4(SO_4)_6(OH_2) \cdot 20H_2O$], K-Jarosite [$(K,H_3O)Fe_3^{3+}(SO_4)_2(OH)_6$]. In general when mining pumps are withdrawn from dewatered workings the rising water will flush these highly soluble minerals into solution, inevitably leading to poor water quality along with acidity generated by rapid hydrolysis of the high metal loadings (so-called 'acid mine drainage').

Sherwood (1997) has successfully modelled the subsequent initial water table rebound regionally and also simulated water flows in the East Fife Coalfield following abandonment and switch-off of pumps in 1995 (Table 1). The water bodies of the flooded mineworkings of the collieries are represented as a series of 'ponds' (also termed 'basins' in Scotland or 'pools' in the USA) connected by pipeflows through e.g. roadways working the major seams and identified in mine plans. For the Frances shaft specifically, 4 'insets' (openings to roadways) are identified in addition to an infilled, closed roadway in the Dysart Main (Table 2). Although the insets might be identified with the level of the given seams, the Lethamwell seam for example was not in fact widely worked and the roadway likely connects instead via inclines to the Dysart Main workings nearby (reflecting strong W–E dips for this major worked seam).

Recharge to the colliery 'ponds' is primarily by surface infiltration of rainfall, except for the offshore areas of the Frances, Michael and Wellesley Ponds (Fig. 1) where a component of seepage from the sea might be expected. The Frances Colliery then connects directly and feeds water flow to the neighbouring Michael Colliery potentially at two levels (Younger, 1994, Fig. 2; Table 2). Frances Colliery is linked also to the adjoining Randolph, Balgonie and Wellesley Pits, especially the former since a mined connection exists between Randolph Pond and the Frances Colliery again working the Dysart Main Seam (Table 2). Although the Barncraig Seam again connects the colliery at >500 m below ground (Younger, 1994) the connection is well away from the Frances shaft and reached by internal declines.

Shortly after the final cessation of all pumping in the East Fife coalfield at the end of 1995, and during the initial period of slow water table recovery a couple of years later, electrical conductivity and temperature depth profiles in the Frances shaft were made by site operators. The recovering water body showed an active influx of water of distinct quality at c. −221 m AOD (c. 270 mbgl). Depth sampling (Nuttall et al., 2002b, their Fig.10; Nuttall and Younger, 2004, their Fig.3) further showed a strongly developed chemical stratification arising

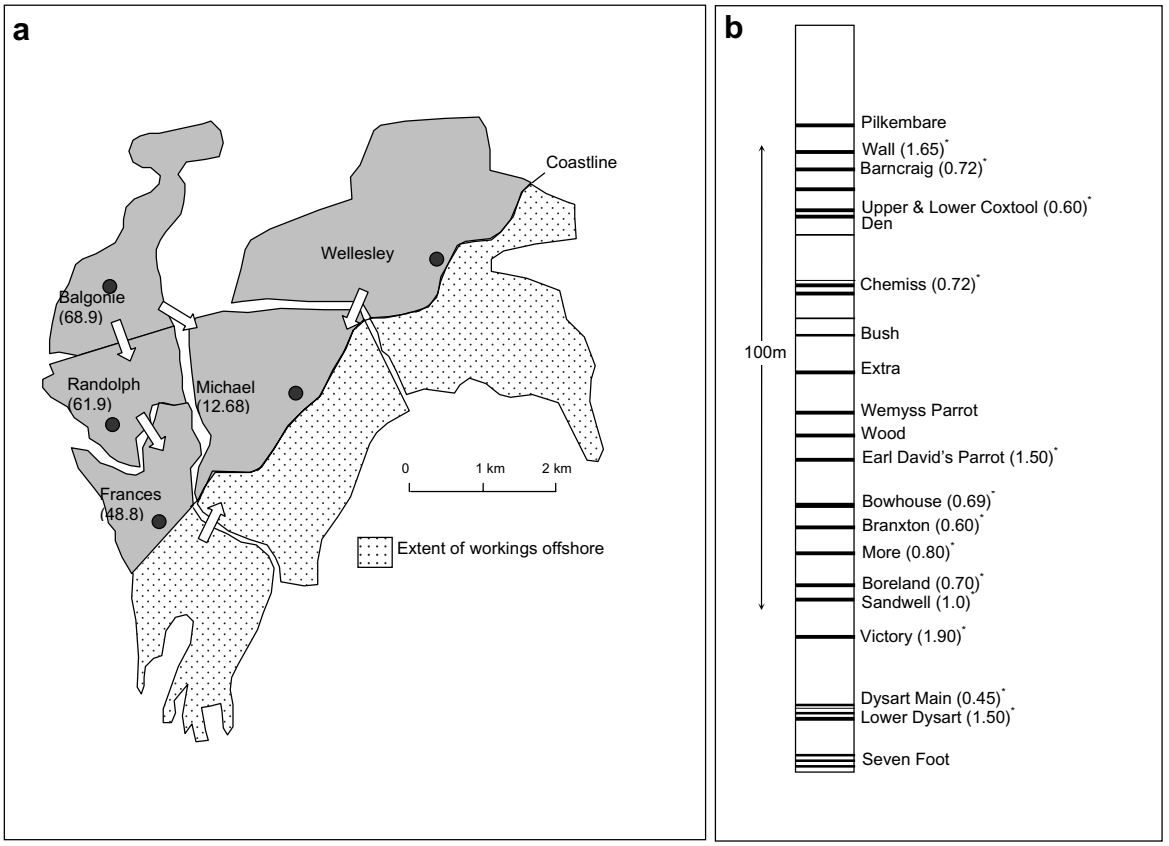

Fig. 2. (a) Map showing the now abandoned collieries in the East Fife Coalfield, emphasising the major mines adjoining Frances Colliery. Filled dots show positions of main shafts with heights above Ordnance Datum (mOD). Shaded areas are those underlain by onshore old workings; stippled areas show the extent of offshore workings. Arrows show the general direction of water movement and approximate position of interconnection between each colliery (after Sherwood, 1997). (b) Generalised Westphalian coal seam sequence for East Fife (after Knox, 1954) showing % S contents of the seams as reported at Frances Colliery (data supplied by British Coal in 1994). Values >0.5 (%S) represent a significant acid-generating potential. Although not shown here the Lethamwell seam deeper in this sequence has 0.7% S (Younger et al., 1995, their Fig. 1; Nuttall et al., 2002a, their Table 4.8).

Table 1
Chronology of the major events relevant to the Frances Colliery

Date	Event
Late 19th century	The coastal Frances (1878) and adjoining (1892) Michael Collieries sunk in the East Fife Coalfield. Start of active works and a programme of dewatering the worked collieries. The principal worked reserve was the Dysart Main seam >8 m thick in places and extending offshore under the Firth of Forth (although such works proved prone to spontaneous collapse)
Late 20th century	Production stops at Michael (1967) and Frances (1985) Collieries
1984–1985	General Miners' Strike nationally. Subsequently very little other than maintenance operations in the East Fife Coalfield. The collieries effectively are mothballed but with dewatering pumps still working
1988	Deep mining finishes in the East Fife Coalfield
December 1995	Operational pumping to dewater the coalfield ends. This marks the beginning of regional-scale water table recovery (rebound) through the interconnected subsurface workings. A legal agreement signed at the time of closure stipulated for the Frances shaft that when the recovering minewaters reached −56 mAOD dewatering by pumping should be restarted to control waters and prevent uncontrolled gravity-flow discharges at the surface (Nuttall and Younger, 2004)
2000	Initial dynamic step-drawdown tests commissioned by the UK Coal Authority to help identify the pumping rate needed to achieve a controlled, steady state in water levels in the Frances shaft. An ancillary aim was to monitor any changes in water quality during pumping

Table 2
Details of insets and connections in the Frances shaft (after: Younger, 1994; Nuttall et al., 2002b; Nuttall and Younger, 2004)

Insets in Frances	Depth (mbgl)	Depth (mAOD)	No. of open roadways at shaft	Comment
Lower Sandwell	115.79	−66.96	1	
Lower Dysart	188.94	−140.11	2	
(Dysart Main)	263.83	−215.00	–	Infilled with Lochead wastes
Lethamwell	270.72	−221.89	2	
Pit Bottom	282.18	−233.35	1	
Connection to	Depth (mbgl)	Depth (mAOD)		Comment
Randolph	88.42	−39.62		Direct connection
Michael	263.83	−215.00		Dysart Main via infiltration through Lochead wastes infill
Michael	566.83	−518.00		Barncraig seam via seepage through 36 m barrier (?)

mbgl: metres below ground level; mAOD: metres Above Ordnance Datum.

in water quality, the top 200 m of the water column showing better quality (typically: Fetot $\leqslant$ 10 mg/L; pH 7; electrical conductivity 3000 μS/cm) than the deepest 70 m ($Fe_{tot} \geqslant$ 599 mg/L; pH 5; electrical conductivity 20,300 μS/cm). Johnson et al. (2004) suggest that since several shafts across the East Fife coalfield similarly show such chemical stratification this phenomenon should be seen as a characteristic of mine ponds *per se* and not just particular to shafts. The depth of active inflow in the Frances shaft was identified by Nuttall and Younger (2004, their Fig. 3) as being at the level of the Lethamwell inset, but is more likely related to the extensive Dysart Main workings which run through to Randolph (Nuttall et al., 2002a,b).

The Dysart Main coal seam in the Frances Colliery has an average total sulfur content of c.0.45% S (Fig. 2; Nuttall and Younger, 2004), just below the threshold of 0.5% S for a significant acid-generating potential. However, the same seam in Randolph has an even higher content (~2.75% S) which would generate poor water qualities (cf. Younger, 2001, his Table 1). Nuttall et al. (2002b) cite that the water pumped from the Randolph pit during active operation was acidic enough (circa pH 5; Fe $\leqslant$ 700 mg/L; Nuttall et al. (2002b), their Table 4.9) that it attacked metal fixings on workers' boots. The mine spoil heap (so-called 'bing') at Randolph also generated significant acidic drainage (cf. Younger, 2001, his Table 1) until it was buried during restoration of an opencast coal mine nearby. Other seams with significant acid-generating potential do exist in the Frances Colliery itself (Fig. 2), but generally these were not developed to the extent of the Dysart Main workings (cf. Knox, 1954); as unmined Coal Measures strata generally have low hydraulic conductivity, abandoned coalfield hydrogeology typically is dominated by the mined voids and workings (Younger et al., 1995).

Hydraulically, Johnson et al. (2004, their Fig. 2.2) point to the flatness of the water recovery curve observed initially in Randolph Pond to infer that when rebound occurred in the coalfield and the Randolph decant point was reached this pond was actively draining into unfilled workings such as Frances and Michael. However, a water balance estimate for the possible contribution of Randolph Pond waters directly to Frances through the mined seam connections has been put at only 10%, even under dewatering conditions during active mine operations (Sherwood, 1997). With water table rebound in Frances it is to be expected that the hydraulic gradient between the two ponds would lessen, and even could be reversed. This could lead to flooding waters in Frances then coming in contact with parts of the Dysart Main seam back towards Randolph (and the poorer S-contents of the seam). These waters in turn would be drawn back to Frances however on resumption of active pumping in the shaft.

After the cessation of pumping in 1995, water levels in the Frances shaft recovered from an initial level of about −223 mAOD, reaching −56 mAOD by the beginning of May 2000, and prompting the need for resumption of active pumping in the shaft (Table 1). At the time the site operators hoped simply that if the recovering mine water was pumped at a relatively high level in the shaft then the stratum of better quality water at the top of the shaft water column could be drawn off without entraining the

poorer water from depth. As the −56 mAOD water level limit was being approached test pumping then was commissioned by the UK Coal Authority to help identify the pumping rate needed to achieve a controlled, steady state in water levels. An ancillary aim was to monitor any changes in water quality occurring during active pumping and identify any further controls necessary. The pump depth of 150 mbgl (∼−100 mAOD) therefore was set at a relatively high level in the Frances shaft, which it was hoped then would pump only the better quality top waters to control the water table.

The initial dynamic step-drawdown tests (Table 3) subsequently reported by Nuttall et al. (2002a,b) and Nuttall and Younger (2004), were attempted during two periods 10/05-30/05/2000 (Pump Test #1 – a single step drawdown) and 07/08-24/09/2000 (Pump Test #2 – three steps drawdown). Pumped mine water was discharged on site into two purpose-built surface treatment lagoons, whence it was discharged to the North Sea (Firth of Forth). These surface treatment lagoons had been constructed initially from compacted clays and colliery spoil material found on site. However, during Pump Test #1 there was apparent recirculation of water back into the shaft through leakage from the lagoons, evidenced by anomalous water level responses during the drawdown phase (cf. Nuttall et al., 2002a, their Fig. 4.13), and it was found that poor water quality rapidly "broke through". Indeed, Nuttall et al. (2002a) report that on the first filling of the lagoons the water drained away, presumably to the shallow subsurface workings causing water to return to the shaft after having first soaked through the colliery spoil lining the lagoons with consequent dissolution of oxidation crusts (cf. Younger, 2001; Hoth et al., 2005; Munk et al., 2006). Subsequent hydraulic analysis of the continued pumping during Pump Test #1 suggested, however, that the effects of Fe(II)-hydrolysis and subsequent Fe(III) ochre deposition (cf. Clarke et al., 1997) and settlement in these lagoons gradually blocked some flow paths such that these surface lagoons were beginning to self-seal. Nevertheless, after only one month of continuous pumping the original planned step test for this first experiment (Pump Test #1) was aborted, as the hydraulic testing had been compromised. The lagoons then were more thoroughly-lined for the second pump test (Pump Test #2).

Nuttall and Younger (2004) have summarised the hydraulic effects observed in the second test pumping (Pump Test #2) of the shaft, and also have described some of the accompanying gross changes in the major element hydrochemistry and water quality. Whilst the initial pumped water observed over several hours of continuous pumping was of reasonable quality as anticipated, subsequent recovered samples again reflected very poor quality waters. Because by Day 5 one of the surface lagoons still had not finished being lined, Pump Test #2 was switched off over a 10-day period until lining was completed, and then drawdown testing resumed (see Figs. 3–6). Hydraulic analysis of the stepped Pump Test #2 data suggested then that in the Frances system there were substantial components of turbulent flow to the shaft during pumping of the extensive open mined voids (Nuttall et al., 2002b, their Table 3).

In the light of this pump testing and the observed water quality changes, Nuttall and Younger (2004, their Fig. 5; Table 4) outline a possible conceptual model of the development of the chemical quality stratification in the recovering water column of the abandoned Frances shaft during rebound, and the effects of the initial stage of active pumping. The phenomenon of the relatively rapid breakdown of stratification on initiation of active pumping in the Frances shaft was observed within 24 h (after one shaft volume removal during pumping tests), and the drastic changes in water quality have been simulated by Nuttall and Younger (2004, their Fig. 6)) to occur within just 16 h of pumping based on simple mixing calculations using observed (standing) initial top and bottom water qualities (prior to pumping) as the end-members.

Table 3
Different stages of the step-drawdown tests performed at Frances Colliery (from: Nuttall et al., 2002a; Johnson et al., 2004, their Fig. 2.2)

Test #	Step	Pump discharge (L/s)	Period	Water level (m AOD)
1	1	38	10/05 09:00-30/05/ 13:30	−57.252 to −57.766
2	1	38	07/08 11:00-04/09 16:30	−54.411 to −55.573
2	2	65	04/09 16:30-19/09 11:15	−55.573 to −56.591
2	3	76	19/09 11:15-23/09 14:00	−56.591 to −56.746

AOD: Above Ordnance Datum.

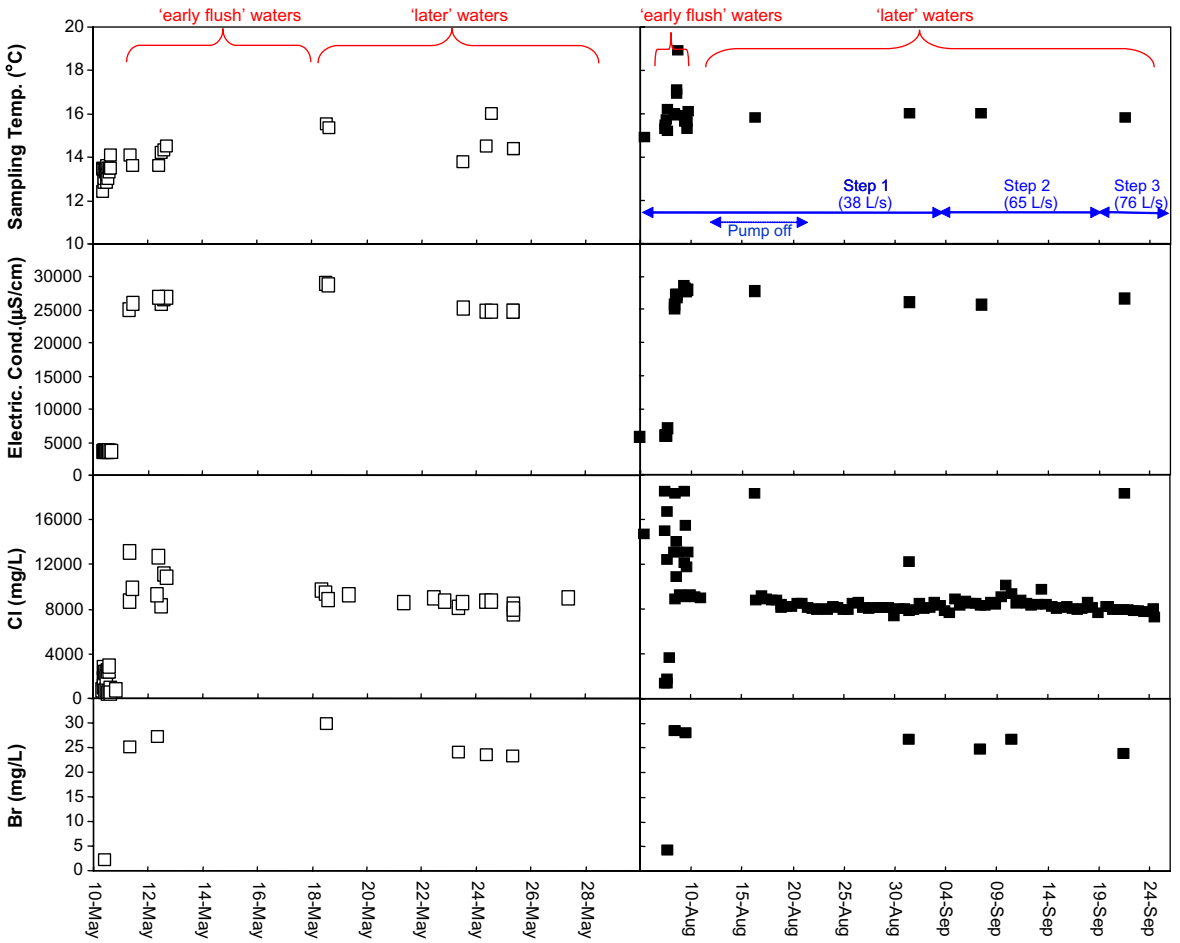

Fig. 3. Monitoring of continuously-pumped water samples from the Frances mineshaft for field parameters (sampling temperature, specific electrical conductivity) and measured dissolved conservative major anions (Cl, Br) during Pump Test #1 (open square) and Pump Test #2 (filled squares). Note the peak concentrations of (Cl, Br) occurring in the early waters (after initial breakdown of stratified waters in the shaft) which are subsequently diluted by following, later waters. The periods of 'early flush' and 'later' waters are identified at the top of the diagram; the stepped pumping regime for Pump Test #2 is also identified.

The further impacts of water drainage and recycling from the surface lagoons postulated from hydraulic testing complicate somewhat this simple conceptual model beyond the initial pumping effects (Table 4). The current paper looks then at characterising its impacts and the further longer-term evolution of water qualities and their possible sources during the extended pumping of the Frances shaft undertaken to test hydraulic control of water levels in the flooded mine. A planned, complementary suite of samples for major and trace element hydrochemistry, (C, H, O, S) isotopic analyses, and age indicators (^{13}C, ^{14}C, ^{3}H) therefore was collected specifically to help elucidate the system and water quality dynamics. Inverse geochemical modelling also has been used to better constrain the water sources and water-rock interactions.

2. Methodology

All samples represent pumped minewaters from the Frances shaft collected during the two separate dynamic step-drawdown tests (Table 3). Pumping test details are outlined in Nuttall and Younger (2004). The "grab" samples were collected at daily to weekly intervals during the continuous pumping schedule, and therefore represent instantaneous flux-averaged concentrations reflecting the zones of contribution (ZOCs) and following the expanding zone of influence (ZOI) of the pumped shaft

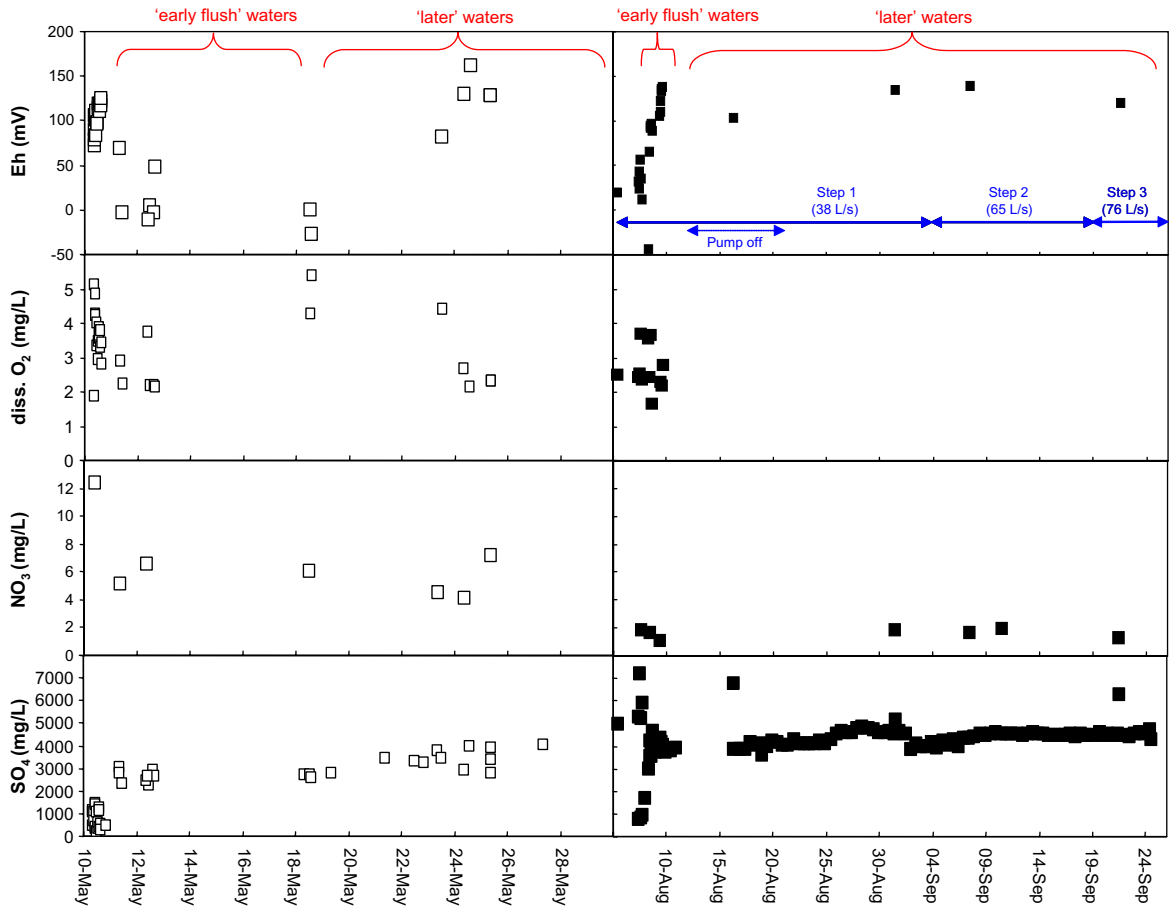

Fig. 4a. Monitoring of continuously-pumped water samples from the Frances mineshaft for field redox parameters (Eh, DO) and the measured dissolved redox-sensitive anions (NO_3, SO_4) during Pump Test #1 (open square) and Pump Test #2 (filled squares). The periods of 'early flush' and 'later' waters are identified at the top of the diagram; the stepped pumping regime for Pump Test #2 is also identified.

after initial removal of storage from the shaft. A single pumped sample was collected also from a borehole near the Randolph shaft on 24/05/2000 (during Pump Test #1).

Field redox parameters (Eh, DO), specific electrical conductivity, pH and sampling temperature were determined at the point of sampling using a Myron 6P Ultrameter and standard electrodes, and a YSI 95 model dissolved oxygen meter. Bicarbonate alkalinity determinations were made on-site trimetrically using a HACH© digital titrator kit. Only field pH and alkalinity determinations for the specific samples discussed in detail in this paper are reported directly in Table 5 to complete the chemical balance, but generally each field parameter was monitored at the times of sampling during the continuous pumping (Charlotte Nuttall, *pers. comm.*).

Major and minor anion concentrations were determined on unacidified water samples in the QUB Environmental Engineering Research Centre (EERC), using a Dionex GP50 gradient elution Ion Chromatograph (IC) equipped with a CD20 conductivity detector. Limits of Determination (LOD, mg/L) are SO_4 (0.02), Cl (0.01), NO_3 (0.02), Br (0.03), F (0.01), respectively. A complementary suite of major and minor cations (including specifically metal analyses: total Fe, Mn and Al by a Unicam 929 Flame Atomic Absorption Spectrophotomer) were determined on acidified samples (<pH 2), with IC (DX-100) and ICP-MS at the University of Newcastle. Cation results and colorimetric Fe(II) analyses (ferrozine method) were provided by Charlotte Nuttall (*pers. comm.*). In all cases samples were filtered prior to analyses using a 0.2 μm filter. Fe^{3+} is estimated by difference (=[Fetot-Fe(II)]).

'Specific' $\delta^{13}C$ (‰, reported relative to the Vienna Pee Dee Belemnite, VPDB, standard) analyses of the Total Dissolved Inorganic C (TDIC) were

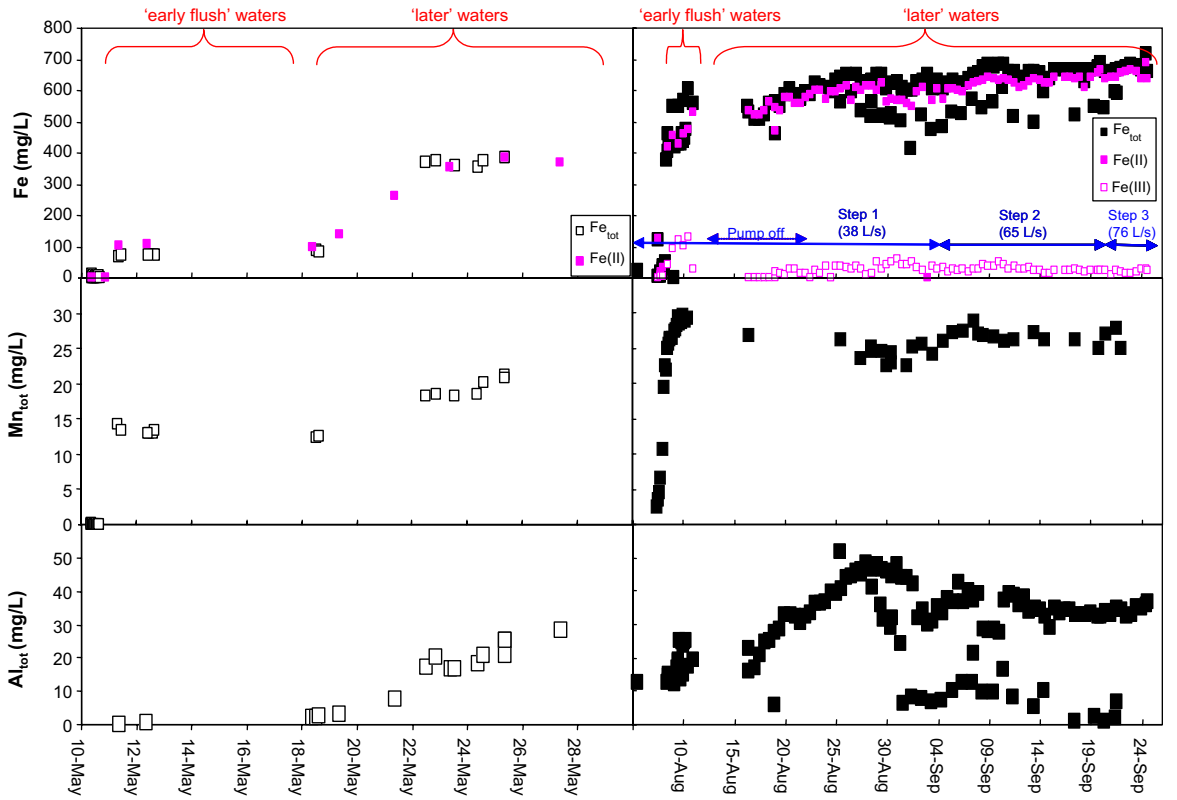

Fig. 4b. Monitoring of continuously-pumped water samples from the Frances mineshaft for measured dissolved redox-sensitive metal-loading (Fe, Mn) and also pH-sensitive Al during Pump Test #1 (open square) and Pump Test #2 (filled squares). Note particularly that Fe_{tot} and SO_4 concentrations (Fig. 4a) appear closely correlated. The periods of 'early flush' and 'later' waters are identified at the top of the diagram; the stepped pumping regime for Pump Test #2 is also identified.

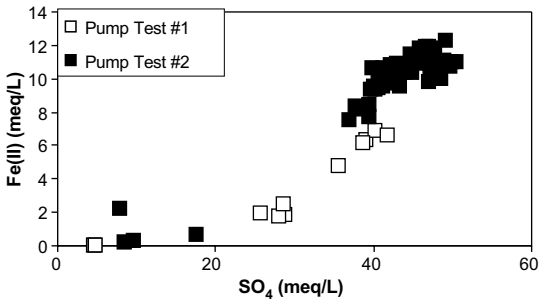

Fig. 4c. Cross plot of (0.45 μm-filtered) dissolved Fe(II) and SO_4 concentrations (meq/L) in water samples taken during continuous Pump Test #1 (open squares) and Pump Test #2 (filled squares). For $SO_4 > 25$ meq/L the relationship with Fe(II) strongly suggests a slope ~2 presumably reflecting the stoichiometry of the products of FeS_2 oxidation. Note that these plotted concentrations have not been adjusted for the effects of a seawater mixing source ($SO_4 = 2710$ mg/L).

made in the EERC at QUB by GC-IRMS on 100 mL crimp seal vial samples that had been poisoned with a few drops of $HgCl_2$ to inhibit any microbial activity during sample storage. These values are preferred for defining the ^{13}C content over bulk measurements (see below) as the latter may be affected by incomplete precipitation leading to enriched values (cf. Table 6b).

For stable isotope analyses of water, 28 mL crimp seal/butyl septum vial samples filled to the brim were analysed for $\delta^{18}O$ in the EERC at QUB by continuous flow Gas Chromatography–Isotope Ratio Mass Spectrometry (GC–IRMS) on a PDZ Europa 20-20 IRMS with gas preparation on a PDZ Europa Anca TGII module and after GC separation on a Chrompack HP6890 with Poraplot-Q capillary column. δ^2H of the water samples was analysed at the Micromass Laboratories in Manchester, UK, by EA-IRMS using a Eurovector Elemental Analyser interfaced to a Vacuum Generators (VG) IsoPrime stable isotope mass spectrometer. Samples either dropped or injected into the chromium reactor immediately decompose, producing H_2 gas which is then introduced online to the IsoPrime for $^1H/^2H$ analysis. Isotopic analyses for $\delta^{18}O$, δ^2H (‰) of water

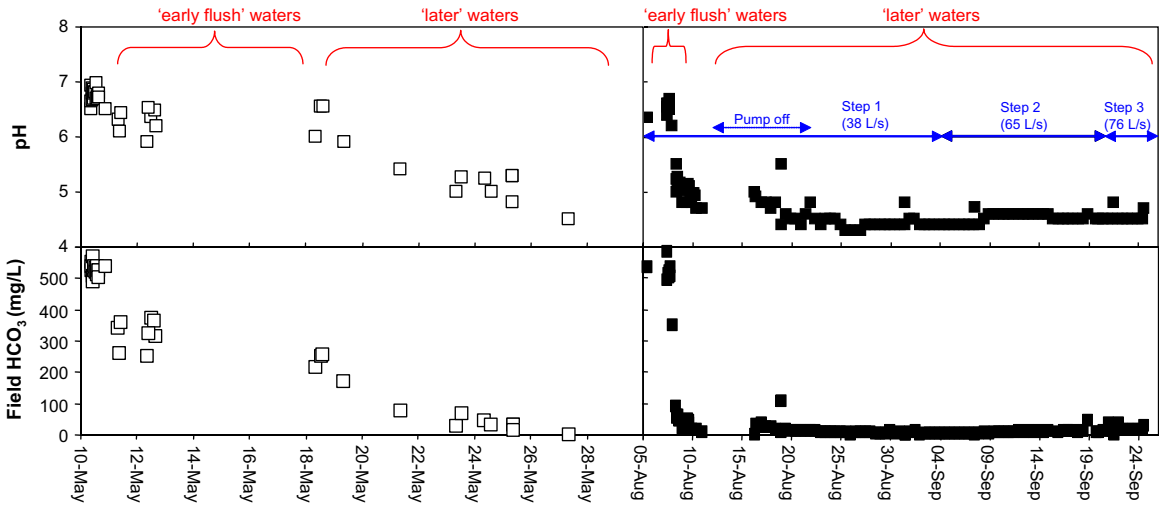

Fig. 5. Monitoring of continuously-pumped water samples from the Frances mineshaft for field pH and dissolved bicarbonate alkalinity during Pump Test #1 (open square) and Pump Test #2 (filled squares). The periods of 'early flush' and 'later' waters are identified at the top of the diagram; the stepped pumping regime for Pump Test #2 is also identified.

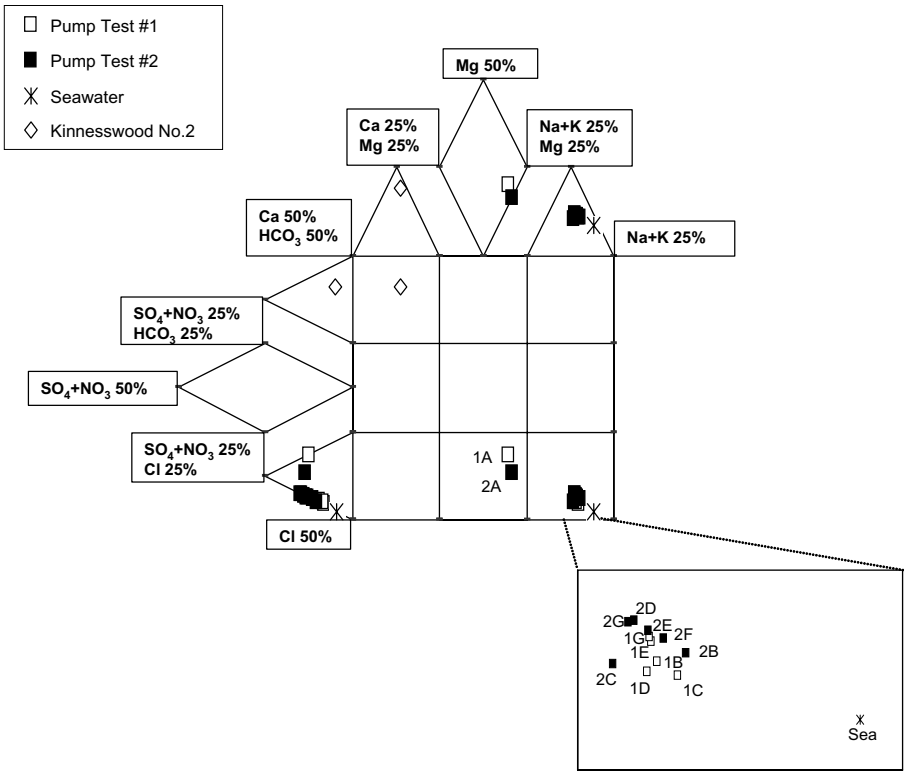

Fig. 6. Hydrochemical (expanded Durov) plot of continuously-pumped water samples from the Frances mineshaft for Pump Test #1 (open squares) and Pump Test #2 (filled squares). A preliminary assessment of the major processes affecting the hydrochemistry may be made using such a plot (Lloyd and Heathcote, 1985). All ion concentrations were converted to meq/L for subsequent plotting of relative ion compositions. A representative sample (Kinnesswood No. 2; McNeill et al., 2003) of recharge water in the Fife Sandstone aquifer is included in this plot. The exploded section shows the relationship between the seawater signature and the pumped water samples in the bottom right-hand quadrant of the Durov plot. 'Early flush' waters are characterised as samples 1B–1D (Pump Test #1) and 2B–2C (Pump Test #2); 'later' waters are characterised as samples 1E–1G (Pump Test #1) and 2D–2G (Pump Test #2).

Table 4
Conceptual sequence of postulated events following mine abandonment leading to initial stratification in water qualities in the Frances shaft and subsequent breakdown as active water pumping resumes (after Nuttall and Younger, 2004)

Stage	Comment
(i) Immediately after pumps switched off	As the water table rebounds naturally, the inflow of contaminated waters from adjacent workings through interconnection(s) at depth leads to poor quality waters initially restricted to the bottom of the shaft. This leads to better water quality then overlaying due to ''fresh recharge'' cascading from shallow, perched aquifers above – i.e. stratification
(ii) Rising water level reaches other connections	As the rising water table reaches higher connections and roadways to other workings, turbulent flows are induced and there may then have been periods of breakdown in this initial water quality stratification (i)
(iii) Stabilisation of flows in the shaft	As the recovering water level fills adjacent workings, the flows stabilise and stratification then could redevelop (as evidenced then in the depth samplings of Frances shaft waters before start of active pumping)
(iv) Active pumping of the shaft	With active, pumping of the shaft waters, the pumped water quality initially reflect the better quality, stratified water body near the top of the shaft – but after one shaft volume is turned over turbulent flows in the interconnected system induced now by the dynamic pumping regime lead to mixing of all the water in the shaft and a consequent poor water quality overall in subsequent recovered samples

Table 5
Major and minor ions – Frances waters (all values mg/L, except pH units)

Sample #	Date	Field pH*	Field HCO_3*	Cl	SO_4	NO_3	Br	F	HS
	Pump Test #1								
1A	10-May-2000	6.94		790	475	12.39	2.02	0.00	0.003
1B	11-May-2000	6.30	341	12071	2109	5.13	25.05	0.00	0.005
1C	12-May-2000	6.53	324	9495	2359	6.56	27.15	0.00	0.050
1D	18-May-2000	6.55	251	13787	2704	5.99	29.80	0.00	0.005
1E	23-May-2000	5.26	68	10793	3121	4.51	23.95	0.00	0.306
1F	24-May-2000	5.25	46	10423	3084	4.13	23.47	0.00	0.005
R	*Randolph Shaft (24 May 2000)*	–	–	34.1	152.9	1.13	0.00	2.78	–
1G	25-May-2000	5.28	30	10261	3130	4.72	200.00	0.00	0.005
	Pump Test #2								
2A	07-Aug-2000	6.40	494	1364	557	1.84	4.28	0.26	0.005
2B	08-Aug-2000	5.51	91	9369	3519	1.67	28.31	0.00	0.012
2C	09-Aug-2000	5.02	37	11193	3859	1.05	27.91	0.00	0.015
2D	31-Aug-2000	4.81	0	9374	4103	1.79	26.72	0.00	0.008
2E	07-Sep-2000	4.71	0	8567	3851	1.63	24.63	0.00	0.005
2F	10-Sep-2000	–	–	–	3241	1.90	26.67	0.00	0.029
2G	21-Sep-2000	4.80	0	9627	4080	1.26	23.73	0.00	0.005

* University of Newcastle values.

(H_2O) are reported relative to Vienna Standard Mean Ocean Water (VSMOW).

$\delta^{18}O$ (‰, w.r.t. VSMOW) and $\delta^{34}S$ (‰, w.r.t. Canyon Diablo Troilite, CDT) of the dissolved SO_4 were also performed at Micromass Laboratories in Manchester, UK. Sulfur isotopic analyses were performed on samples that had been collected in 1-L air-tight Nalgene bottles, filled to the brim and poisoned in the field with a few drops of $HgCl_2$. The dissolved SO_4 samples were directly precipitated as $BaSO_4$ following the method of Carmody et al. (1998). Subsequently samples were analysed by CF-IRMS on an Optima (Micromass UK Ltd., Manchester, UK) stable isotope ratio mass spectrometer coupled in Continuous Flow mode to an elemental analyser (NA 1500, Carlo Erba Strumentazione, Milan, Italy). Flash combustion of the sample in the presence of O_2 at a temperature of 1800 °C was followed by a Cu reduction stage at 800 °C which ensured total conversion of any SO_3–SO_2. The mass spectrometer was set to monitor the sulphur dioxide $^{32}SO_2/^{34}SO_2$ isotopes at m/z 64 and 66.

Tritium activity (^3H, Tritium Units – 1 TU $^3H/Hx10^{18}$) determinations were made at the

Laboratory of Isotope Geosciences, University of Arizona (USA) on 1-L air-tight Nalgene plastic bottle samples after a standard electrolytic enrichment method for water and correction back to the sampling date. The detection limit for a 1500 min count, 8× enrichment is quoted as being 0.9 TU. Radiocarbon (^{14}C) determinations were made by tandem accelerator mass spectrometry (TAMS) in the NSF Accelerator Mass Spectrometry Group, University of Arizona (USA). At the QUB EERC, 1-L air-tight Nalgene plastic bottle samples were treated by pH adjustment to >11 by addition of 8 mL of 2.5 M carbonate-free NaOH. Approximately 5–6 g $BaCl_2$ was then added to precipitate the Total Dissolved Inorganic C (TDIC) as 'bulk' carbonate under closed conditions from atmospheric CO_2. Subsequently the precipitate was placed under vacuum and acidified with H_3PO_4 to evolve CO_2 gas. An aliquot of the gas then was collected and analysed in the EERC for $\delta^{13}C$ (‰) of the CO_2 (reported against the VPDB standard) on a Vacuum Generators (VG) PRISM III dual-inlet, high precision, magnetic sector mass spectrometer. Further gas aliquots were then sent to the NSF facility for $^{14}C/^{13}C$ determination after conversion of the evolved sample CO_2 to a graphite source by TAMS analysis. ^{14}C results are reported as per cent modern carbon (pmc) activities.

3. Results

Major/minor ion results are presented in Table 5, with isotope analyses presented in Tables 6a and 6b. Field sampling temperatures for the Frances waters in Pump Tests #1 and #2 initially were 13.5 °C and 14.9 °C, respectively, enhanced over typical shallow groundwater temperatures of 10 °C in the region; an average UK geothermal gradient of ~26 °C/km would suggest a sampling depth ~150 m, in line with the actual depth of the pump. However in both Tests (#1 and #2) during pumping the sampling temperatures increased slightly over start conditions (Fig. 3) and remained relatively enhanced by ~1 °C throughout, presumably reflecting the mixing-in of a relatively deeper-sourced water component, although an initial spike of temperature seen in Pump Test #2 suggests possible sensitive impact of seasonally warmer surface waters or the effects of exothermic acid mine drainage reactions (lagoon waters?).

Full water chemical analyses generally fall within the range of ±5% Charge Balance Error (CBE). In terms of mineral saturation indices using NETPATH (Plummer et al., 1994) and WATEQ4F (Ball and Nordstrom, 1991), all waters remain undersaturated with respect to the common carbonate minerals calcite [$CaCO_3$] and dolomite [$MgCO_3$]. Based on the field measured redox (Eh) values, speciation calculations suggest that siderite [$FeCO_3$] and rho-

Table 6a
O, H, S isotope systematics of H_2O and SO_4 – Frances waters (all δ-values ‰)

Sample #	Date	$\delta^{18}O$ (VSMOW)	+/−(1SD)	$\delta^{2}H$ (VSMOW)	+/−(1SD)	$\delta^{18}O(SO_4)$ (VSMOW)	+/−(1SD)	$\delta^{34}S(SO_4)$ (CDT)	+/−(1SD)
	Pump Test #1								
1A	10-May-2000	−6.7	0.0	−30.4	0.35	4.5	0.1	1.38	0.44
1B	11-May-2000	−3.5	0.2	−28.4	0.21	6.6	0.1	13.58	0.15
1C	12-May-2000	−3.6	0.0	−28.9	0.18	6.2	0.1	13.51	0.18
1D	18-May-2000	−3.1	0.0	−26.1	0.52	5.9	0.1	13.38	0.09
1E	23-May-2000	−3.8	0.3	−31.0	0.46	3.5	0.1	10.75	0.52
1F	24-May-2000	−3.9	0.0	−31.8	0.73	4.1	0.1	10.14	0.28
R	*Randolph Shaft (24-May-2000)*	−3.9	0.2	−31.0	0.54	–	–	–	–
1G	25-May-2000	−3.9	0.0	−32.6	0.17	3.9	0.1	9.84	0.31
	Pump Test #2								
2A	07-Aug-2000	−6.4	0.0	−48.6	0.62	–	–	4.96	0.24
2B	08-Aug-2000	−3.8	0.0	−31.3	0.34	–	–	10.70	0.35
2C	09-Aug-2000	−3.5	0.1	−29.9	0.36	–	–	10.61	0.28
2D	31-Aug-2000	−3.7	0.0	−31.2	0.74	–	–	9.26	0.07
2E	07-Sep-2000	−3.8	0.1	−31.1	0.77	–	–	9.57	0.05
2F	10-Sep-2000	−3.6	0.1	−28.9	0.38	–	–	–	–
2G	21-Sep-2000	−3.9	0.2	−31.0	0.54	–	–	9.34	0.17

Table 6b
^{3}H and C-isotope systematics of TDIC – Frances waters (all δ-values ‰; ^{3}H activity in TU)

Sample #	Date	^{3}H activity (TU)	+/ −(1SD)	$\delta^{13}C$ 'specific' (VPDB)	+/ −(1SD)	$\delta^{13}C$ 'bulk' (VPDB)	+/ −(1SD)	^{14}C (pmc)	+/ −(1SD)
	Pump Test #1								
1A	10-May-2000	12.8	0.63	−10.3	0.5	−3.74	0.04	12.1	0.2
1B	11-May-2000	6.6	0.48	−6.5	0.0	−6.80	0.19	16.5	0.2
1C	12-May-2000	–	–	−6.7	0.0	−5.92	0.00	–	–
1D	18-May-2000	6.1	0.47			−4.19	0.12	17.2	1.0
1E	23-May-2000	–	–	−9.8	0.0	−4.55	0.00	–	–
1F	24-May-2000	6.4	0.46			−1.70	0.29	16.8	0.3
1G	25-May-2000	–	–	−9.8	0.0	−4.57	0.19	–	–
	Pump Test #2								
2A	07-Aug-2000	–	–	−6.8	0.2	−4.52	0.03	–	–
2B	08-Aug-2000	–	–	−6.4	0.1	−6.57	0.18	–	–
2C	09-Aug-2000	–	–	–	–	−7.56	0.06	–	–
2D	31-Aug-2000	–	–	−9.7	0.5	−5.44	0.08	–	–
2E	07-Sep-2000	–	–	−10.8	0.3	−6.36	0.02	–	–
2F	10-Sep-2000	–	–	−11.7	0.0	–	–	–	–
2G	21-Sep-2000	7.1	0.48	−7.3	0.1	−10.30	0.00	36.5	2.2

docrosite [$MnCO_3$] initially appear close to mineral saturation in early waters, but in later waters with high metal loadings become clearly undersaturated. All waters are saturated with respect to gibbsite [$Al(OH)_3$] and goethite [FeOOH] phases, which are thus possible sinks for dissolved Fe and Al, respectively, in this system. All waters remain highly undersaturated with respect to both melanterite and also K-jarosite. Using the Fe(II)/Fe(III) couple rather than possibly mixed signature Eh measurements to speciate other redox components (Nordstrom et al., 1979; Macalady et al., 1990; Grenthe et al., 1992; Nordstrom, 2000) apparently drives K-jarosite mineral saturation indices to be highly saturated (although K-jarosite is not in fact invoked as a necessary source or sink in this paper).

3.1. Mixing indicators (Cl, Br, stable isotopes of water)

Since the Cl^- ion in geochemical terms tends to act conservatively in subsurface waters, concentrations generally can be used as a tracer of water mixing within groundwater systems. The initial water chlorinities of ~800 and ~1300 mg/L (Pump Test #1 and #2, respectively; Fig. 3) recorded at the start of pumping suggest that first samples of the initial standing Frances shaft-waters themselves represent a dilution and/or mixing of a saline component with fresher and better quality water. These first samples reflect the initial diffuse, density-driven stratification of water qualities (since saline waters are denser than freshwater) in the water column existing at the pump tests start-up. Active pumping then shows an initial, rapid breakdown of water quality stratification in the shaft over the first 24 h of pumping (Nuttall and Younger, 2004), leading to poor quality, high salinity waters being pumped from the shaft. However, after the first 24 h of continuous pumping, in both tests the time sequences of Cl-concentrations (Fig. 3) suggest then an 'early flush' of even higher Cl-concentration saline water over and above the effects of the breakdown in stratification in the shaft, and occurring over a period of a few days to one week of pumping. These 'early flush' waters give the highest Cl-concentrations encountered during pumping, and apparently are associated with the possible leakage of the surface lagoon waters (see below). Subsequent following ('later') waters apparently also have a saline component but samples show a progressively diluted chlorinity signature such that Cl-concentrations generally decrease from the peak value following the 'early flush' phenomenon. These trends are mimicked also in electrical conductivity monitoring and dissolved Br^- (Fig. 3); initial Br^- concentrations of 2 and 4 mg/L are observed to increase to peak values of around 28 and 30 mg/L, respectively, after the first few days of pumping, but with a subsequent slow dilution of these concentrations over the subsequent weeks of continuous pumping. Initial $\delta^{18}O$ values of −6.7 and −6.4‰ (Table 6a) are isotopically heavier than local shallow groundwaters in the Fife region (around −8 to −9‰; McNeill

et al., 2003), confirming that first sampled waters from the shaft at the start of pumping are not simply freshwaters. The stable isotopic signatures then become even heavier after the first day of pumping, with values around −3 to −4‰ in both 'early flush' and following, 'later' waters.

3.2. Redox indicators (Eh, DO, NO_3, Fe, Mn)

During Pump Test #1 (Fig. 4a) Eh values initially increase from c. +70 to c. +150 mV after the start of pumping, presumably reflecting pumping of the shallowest waters and initial breakdown of stratification in the shaft. Values then 'sag' to ~0 mV after the first 24 h of pumping and the postulated influence of induced leakage of reduced waters from the surface lagoons (the identified 'early flush' waters; their reduced nature presumably reflecting reaction of infiltrating waters with the mine spoil initially used to build the lagoons). Dissolved O_2 (DO) contents co-vary with Eh at least initially, decreasing from c. 5 mg/L to around 2 mg/L. The Eh levels recover to values c. +150 mV only after a period of a week or so, possibly reflecting the effect then of self-sealing of the lagoons by ochre precipitates preventing leakage; within this period DO contents also have recovered to c. 5 mg/L. DO apparently decreases again in 'later' pumped waters (Fig. 4a). Pump Test #2 starts with relatively more reduced conditions (c. +20 mV; DO values 2–4 mg/L). Eh again increases over the first few days of pumping to c. +150 mV, and then there is a slight 'sag' after 72 h (including also the period when the pumps were switched off), but subsequent recovery to more oxidised (c. 150 mV) values for the rest of the test.

Other significant chemical changes affect dissolved NO_3 (Fig. 4a), and total Fe and total Mn (Fig. 4b). Nitrate generally decreases over time; however, Pump Test #2 data show significantly lower NO_3 concentrations (ca. 1–2 mg/L) in comparison with Pump Test #1 (initially 12 mg/L in Pump Test #1, decreasing to 4–5 mg/L). Measured Fe_{total} concentrations in both tests reflect predominantly dissolved Fe(II). For Pump Test #1, the apparent Eh 'sag' (Fig. 4a) reflects a period where both Fe_{total} and Fe(II) concentrations have increased in the 'early flush' waters after 24 h pumping from low levels to ca. 100 mg/L (Fig. 4b); concentrations remain at this level over a week of pumping but subsequently there is a significant rise to c. 400 mg/L in the 'later' waters. During Pump Test #2 (Fig. 4b), Fe(II) and also Fe(III) both increase on initial pumping rapidly attaining c. 400 mg/L Fe^{2+} and c. 100 mg/L Fe^{3+}, respectively in the first 72 h of pumping, but then there is a "sag" following Eh (Fig. 4a) and occurring before the surface lagoons were finally lined properly – presumably related to recirculating waters (although not to the same degree apparent in Pump Test #1). Following the stopping and restarting of pumping Fe(III) remains comparatively low whilst Fe(II) and Fe_{total} concentrations slowly increase to c. 700 mg/L over the period of the multi-step test (Fig. 4b). The enhanced Fe(III) at the start of Pump Test #2 suggests some relatively more oxidised waters initially, in line with DO values (Fig. 4a). Dissolved Mn_{tot} concentrations in both pump tests (Fig. 4b) also follow Fe(II) concentrations reflecting a redox control giving concentrations up to ca. 25 mg/L.

The highest metals (total Fe, Mn, Al) loadings appear to be associated with the 'later' phases of pumping on top of the influence of the 'early flush' (lagoon) waters, when dissolved Cl-concentrations are gradually declining (Figs. 4a and 4b). In pump test #1 (Fig. 4b), dissolved Al_{tot} becomes enhanced only after a week or so of pumping - rising to c.30 mg/L; similarly during pump test #2, Al_{tot} concentrations are initially c.10–20 mg/L but significantly rise to >30 mg/L only following the completion of the lining of the surface lagoons and presumably controlled by pH (Fig. 5).

3.3. Sulfur systematics (SO_4, $\delta^{18}O(SO_4)$, $\delta^{34}S(SO_4)$)

Dissolved SO_4 (up to c. 4000 mg/L; Fig. 4a) also apparently follows generally the Fe(II) concentration variations during both pumping tests (Figs. 4b and 4c). Monitoring of SO_4-concentrations for the Frances waters shows an initial steep increase, with a slower rate of increase in the 'later' samples (Fig. 4a). Unlike for Cl and Br there is no apparent dilution of SO_4-concentrations in these 'later'waters (Table 5), implying an internal source and generation of dissolved SO_4; SO_4 concentrations generated in Pump Test #2 apparently are higher than for Pump Test #1. Increasingly the S- and O-isotopes of dissolved sulfur species are being used to identify and characterise the effects of acid mine drainage (cf. Wright and Nordstrom, 1999). Stable isotopic signatures are only available for the dissolved SO_4; samples did not yield enough dissolved sulfide (generally

$HS^- < 1$ mg/L; Table 5). Samples were measured for $\delta^{34}S(SO_4)$ only for the Pump Test #1 samples.

3.4. Age indicators (^3H, ^{13}C, ^{14}C)

Only a limited number of samples were analysed for age indicator parameters (^3H, ^{14}C) during the pumping tests (Table 6b). Monitoring of ^3H activity during Pump Test #1 indicated an initial value in the pumped waters of c. 13 TU. Similar activities have been reported for fresh, shallow groundwaters at recharge in the Upper Devonian Sandstone aquifer in Fife (McNeill et al., 2003). However, pumping of the Frances waters shows a decrease within 24 h to an apparent dynamic equilibrium value of 6–7 TU, i.e. 50% of the initial value.

For the inorganic carbon systematics there is a decrease in HCO_3 alkalinity to low levels over time (Fig. 5) reflecting the neutralisation of acid ($H^+ + HCO_3^- = H_2CO_3$) produced as a result of sulfide oxidation (cf. Eq. (2)). For Pump Test #1, pCO_2 values calculated from thermodynamic modelling increase over the first few days as alkalinity decreases, but then decrease during the 'early flush' phase, recovering only in the 'later' waters. Estimated equilibrium pCO_2values $\sim 10^{-2}$–10^{-1} atm generally are all significantly higher than atmospheric values $\sim 3 \times 10^{-4}$ atm suggesting a closed system. Alkalinity also decreases in the 'later' waters (Fig. 5), and as a corollary there is a pH decrease as the buffering capacity is depleted.

Raw groundwater ages from sample ^{14}C activities (estimated based simply on applying the radioactive decay law for an initial activity of 100 pmc) suggest apparent residence times of thousands of years for all waters, however this is at odds with the presence of ^3H and suggests a predominating effect of mixing (e.g. Mazor et al., 1986) over imprinting and dilution of the ^{14}C signatures by ''dead'' C sources. The decrease in ^3H activity in Pump Test #1 is concomitant however with an apparent increase in ^{14}C activity from initially 12–17 pmc (Table 6b) apparently suggesting a 'younging' of ages. End-member geochemistries, however, are not well constrained for this system, precluding detailed/quantitative modelling of actual geochemical ages (eg. Mook, 1980; Kalin, 2000).

4. Discussion

Samples from both pump tests plot on an expanded Durov diagram generally along the major diagonal axis suggesting simple mixing/dissolution as a predominating process signature (Fig. 6). Many samples plot close to the seawater position. Nuttall and Younger (2004, their Fig. 4) also identify in a Piper plot effectively two end members in the temporal evolution of the major element hydrochemistries for Frances samples: (i) the better water quality with a conductivity ~5000 μS/cm seen at the start-up of pumping and presumed derived mainly from shallow-sourced recharge to the shaft; and (ii) the water pumped at the end of the test which has evolved towards a seawater plotting position. Initially this suggests then a simple two-component mixing between better quality waters and a saline source (potentially seawater).

4.1. Sources of salinity/chlorinity

Samples from both pump tests fall along a similar δ^2H–$\delta^{18}O$ relationship (Fig. 7). The slope of this relationship is similar but the intercept on the *y*-axis (δ^2H) slightly less than for either the Global Meteoric Water Line (GMWL) or an appropriate Local Meteoric Water Line (LMWL; Valentia, Ireland). Isotopic signatures in the pumped Frances waters are also heavier than the average $\delta^{18}O$ and δ^2H values of shallow, recent groundwaters seen e.g. in the Fife Sandstone aquifer (Fig. 7; McNeill et al., 2003). The apparent trendline for the samples from both pump tests gives a *y*-intercept close to zero, again initially suggesting simple two-component mixing between the initial pumped waters and a seawater component, in line with preliminary interpretation of the Durov plot. The $\delta^{18}O$ change during pumping from the initial water signature at start of test suggests then potentially ~40–60% mixing of a seawater source ($\delta^{18}O = 0‰$) with freshwater recharge [Appendix A(i)]. The single sample from the Randolph shaft also plots on this apparent δ^2H–$\delta^{18}O$ mixing line suggesting that its chlorinity too may be from seawater, which is surprising since this colliery lies inland (Fig. 7). However, this interpretation is not supported by the Cl-correlation plot (Fig. 8), and Nuttall (*pers. comm.*) suggests that this $\delta^{18}O$ signature is likely enriched in $\delta^{18}O$ as an artefact of sampling conditions at the Randolph well which proved difficult to purge properly. Nonetheless, the pumped Frances samples apparently all display a certain degree of saline mixing/sourcing of their hydrochemistry from seawater. Younger (1994) points out that molal Mg/Cl ratios in Frances and coastal Michael waters are ~0.1 (confirmed

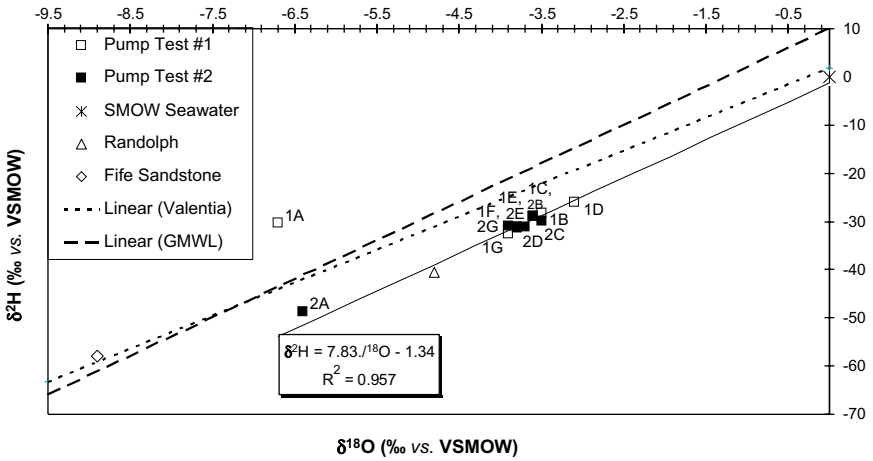

Fig. 7. Genetic cross-plot of stable isotopes of water (δ^2H, $\delta^{18}O$) signatures for the continuously-pumped water samples from the Frances mineshaft for Pump Test #1 (open squares) and Pump Test #2 (filled squares), showing apparent two-component mixing with a seawater source. The Global (GWML; defined as $\delta^2H = 8.\ \delta^{18}O + 10$; Craig, 1961) and Local (LMWL; characterised by the IAEA Global Network In Precipitation (GNIP; http://www.iaea.org/programs/ri/gnip/gnipinfo.htm) data for Valentia, Ireland) Meteoric Water Lines are shown. The single sample collected from the Randolph shaft is plotted (Table 6a) along with an average value for recharge waters to the Fife Sandstone aquifer (McNeill et al., 2003). 'Early flush' waters are characterised as samples 1B–1D (Pump Test #1) and 2B–2C (Pump Test #2); 'later' waters are characterised as samples 1E–1G (Pump Test #1) and 2D–2G (Pump Test #2).

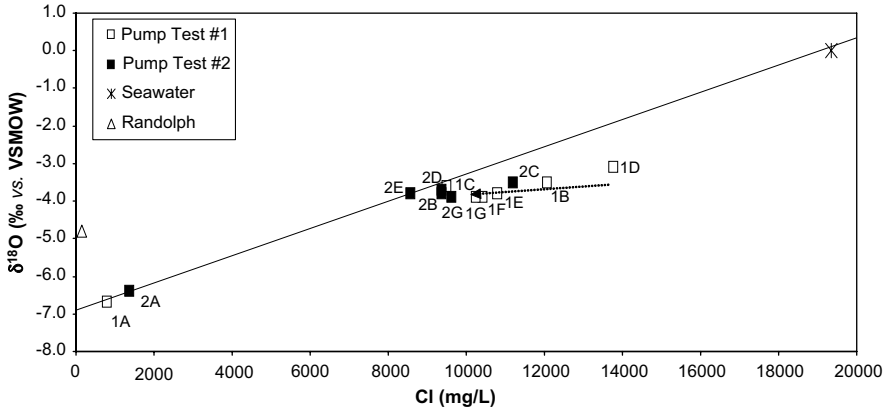

Fig. 8. Chloride correlation-plot of $\delta^{18}O$ stable isotope signatures for the continuously-pumped water samples from the Frances mineshaft for Pump Test #1 (open squares) and Pump Test #2 (filled squares), showing the influence of mixing of freshwater and seawater sources. The single sample from Randolph (Table 6a) is also plotted. 'Early flush' waters are characterised as samples 1B–1D (Pump Test #1) and 2B–2C (Pump Test #2); 'later' waters are characterised as samples 1E–1G (Pump Test #1) and 2D–2G (Pump Test #2). The dotted arrow suggests the trend of the 'later' waters back to the seawater-freshwater mixing line over time.

also in the recent investigation; data not presented), similar to a seawater ratio and significantly different from ratios ~0.0008 in shallow groundwaters and ~0.009 in basin brines as found in deep coal workings in Durham (Edmunds, 1975). This confirms the influence of a seawater signature as a mixing end-member. Moreover, Younger et al. (1995) on the basis of SO_4-concentrations suggested originally that Frances and Michael waters are 30–60% mix of seawater with freshwater, in line with the simple two-component mixing estimate from the stable isotope data.

A cross-plot of $\delta^{18}O$ against sample chlorinity (Fig. 8) shows that samples with chlorinities up to c. 9000 mg/L Cl do plot close to a simple two-component mixing line between a better water quality component ('freshwater') and seawater. The *y*-intercept of the $\delta^{18}O$–Cl seawater mixing line suggests a

dilute initial end-member freshwater with a $\delta^{18}O$ isotopic signature of c. $-7‰$ closer to that for local precipitation in the region (Fig. 7; McNeill et al., 2003). However, looking closely at the time sequence of sampling, the samples plotting close to the mixing line relate generally to the period of 'later' samples taken after peak inputs when the chlorinity subsequently and gradually is being diluted (Fig. 3). For chlorinity samples >9000 mg/L Cl the $\delta^{18}O$–Cl trend becomes significantly flatter, suggesting the influence of another saline component with an enhanced Cl content and $\delta^{18}O$ ~ -4 to $-5‰$. These samples generally are related to the phase of 'early flush' waters occurring in both tests after the first day or so of pumping. Since the $\delta^{18}O$ signatures of these waters do not vary dramatically this suggests either:

(i) That the source of this enhanced Cl end-member is a water component of high salinity which may have a distinctly different $\delta^{18}O$, but where the mixing fraction for the waters is small, or; (ii) that the $\delta^{18}O$ signature is in fact similar to the freshwater–seawater mixing end-member.

The timing of these 'early flush' waters has been identified with induced recirculation of holding waters from the surface lagoons based on water level response in the shaft during drawdown (Nuttall et al., 2002a). This then would explain the similarity in $\delta^{18}O$ for these and 'later' waters. The apparent trend for these most saline 'early flush' waters then intercepts the freshwater–seawater mixing line at c. 9000 mg/L Cl which would imply a mixing end-member with a ~50% seawater signature (taking seawater chlorinity c. 19000 mg/L Cl; Drever, 1997, p. 345), consistent with mixing of an initial fresher water of $\delta^{18}O$ $\sim -7‰$ with seawater ($\delta^{18}O \sim 0‰$) that gives a mass balance, mixed signature around $-4‰$. For these most saline ('early

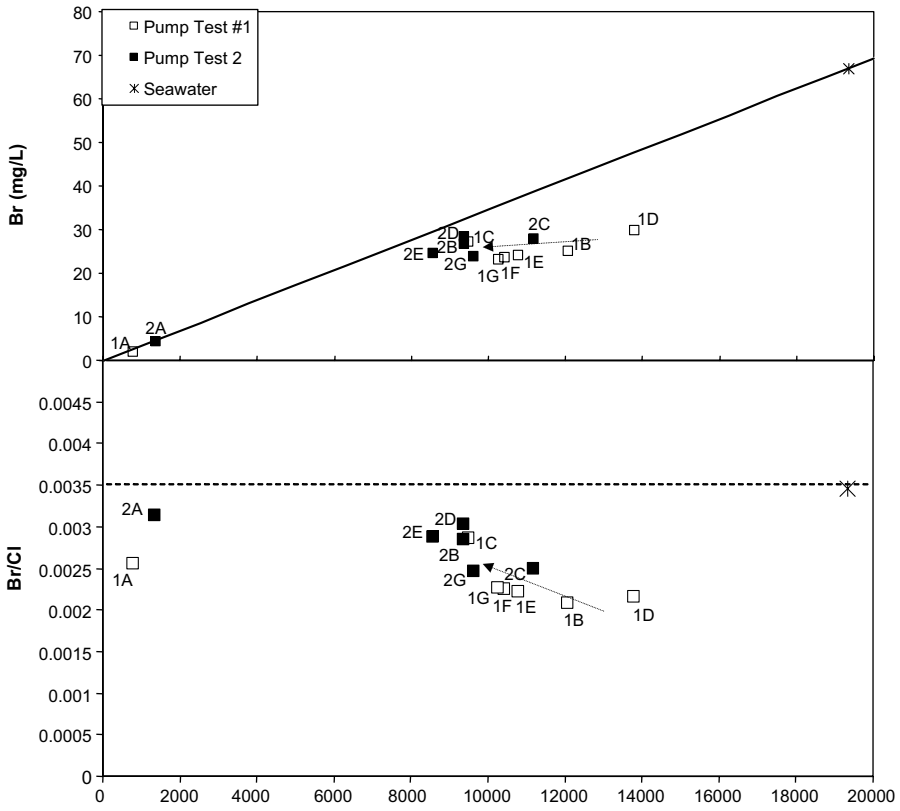

Fig. 9. Chloride correlation-plot of measured Br-concentrations and Br/Cl ratios for the continuously-pumped water samples from the Frances mineshaft for Pump Test #1 (open squares) and Pump Test #2 (filled squares), showing the influence of mixing of freshwater and seawater sources. The single sample from Randolph (Table 6a) is also plotted. The stippled line shows the characteristic Br/Cl (Weight) ratio of 3.45×10^{-3} for modern seawater. 'Early flush' waters are characterised as samples 1B–1D (Pump Test #1) and 2B–2C (Pump Test #2); 'later' waters are characterised as samples 1E–1G (Pump Test #1) and 2D–2G (Pump Test #2). The dotted arrow suggests the trend of the 'later' waters back to the seawater–freshwater mixing line over time.

flush') waters (>9000 mg/L) the evidence points then to a three-component admixture between a component comprising equal proportions of seawater and freshwater, mixing with an enhanced Cl component potentially reflecting the influence of water–rock interaction and/or an evaporitic source linked to recirculation from the surface lagoons. The latter component is likely de-icing salts (eg. rock salt) formerly used in the mine yard.

This second salinity source as evidenced in the 'early flush' waters is picked out also in the Br data. Dissolution of evaporitic minerals such as halite typically would produce enhanced chlorinities having little associated $\delta^{18}O$ and a Br/TDS ratio significantly less than that of seawater; halite dissolution brines typically have a Br/Cl ratio $\sim 1.67 \times 10^{-3}$, in comparison to a modern seawater (weight) ratio of 3.45×10^{-3} (Richter and Kreitler, 1993; Smith, 1991; Hounslow, 1995). A cross-plot of Br against Cl suggests again that the initial saline components at the start of pumping lie close to a simple freshwater–seawater mixing line (Fig. 9). The influence of the evaporitic source again is seen as pumping commences: the most saline ('early flush') waters show a Br/Cl ratio significantly less than that for seawater and closer to an evaporitic source signature; samples having chlorinities ⩽c. 9000 mg/L Cl (including 'later' waters) lie close to the seawater mixing line. The effect is shown clearly in a plot of Br/Cl ratio versus Cl (Fig. 9), where the highest chlorinity 'early flush' saline water samples (>9000 mg/L Cl) suggest a mixing end-member with Br/Cl ~0.002 which then

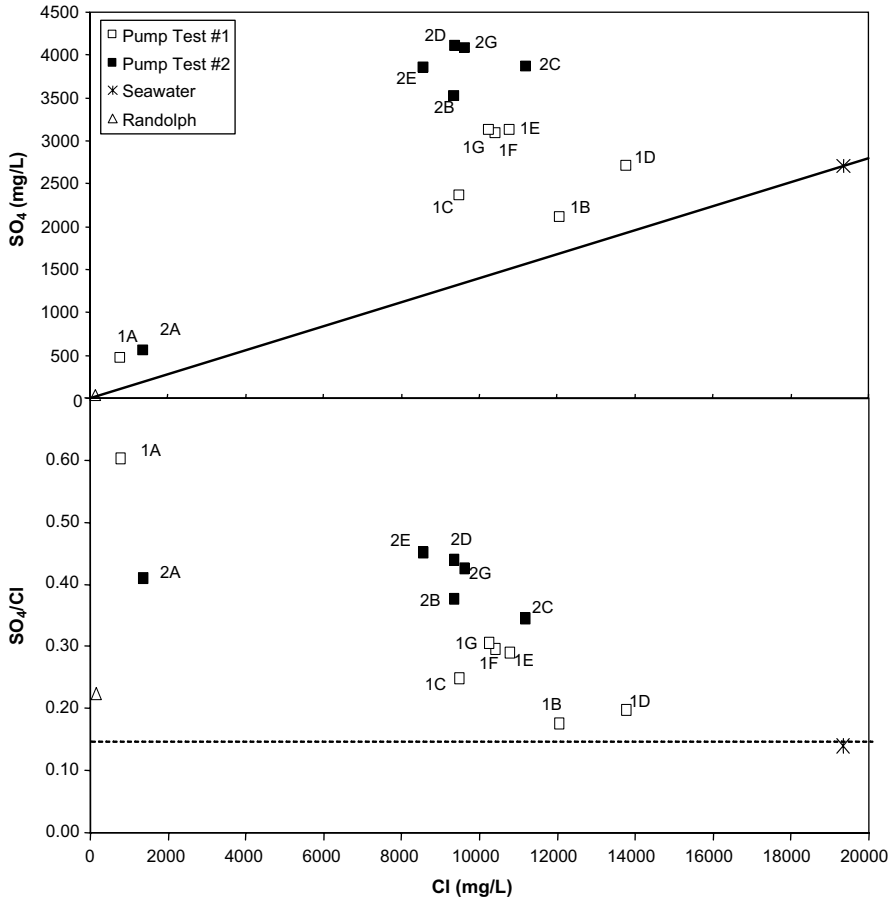

Fig. 10. Chloride correlation-plot of measured SO_4 concentrations and SO_4/Cl ratios versus Cl for the continuously-pumped water samples from the Frances mineshaft for Pump Test #1 (open squares) and Pump Test #2 (filled squares), showing the influence of mixing of freshwater and seawater sources. Note that SO_4 concentrations increase as Cl-concentrations are diluted in the later waters. The single sample from Randolph (Table 5) is also plotted. The stippled line shows the characteristic SO_4/Cl (Weight) ratio of 0.14 for modern seawater. 'Early flush' waters are characterised as samples 1B–1D (Pump Test #1) and 2B–2C (Pump Test #2); 'later' waters are characterised as samples 1E-1G (Pump Test #1) and 2D–2G (Pump Test #2).

in time trends towards the characteristic seawater ratio (Br/Cl ~0.0035) in the 'later' waters as the overall chlorinity becomes more diluted through continuing freshwater–seawater admixture. Linear extrapolation of this trend for the more saline waters from Pump Test #1 waters then suggests an intercept with the freshwater–seawater mixing line of ca. 5000 mg/L or only 25% direct seawater mixing with a freshwater for these 'later' waters, rather than the 50% implied by $\delta^{18}O$.

Overall, therefore, the effect of the 'early flush' waters is seen in the salinity and water quality monitoring during both pump tests and confirms the concerns expressed by Nuttall et al. (2002a) about the possible impact of recirculating waters being induced from leaky lagoons during the hydraulic drawdown tests.

4.2. Acid mine drainage

Regardless of the sources of chlorinity for 'early flush' and 'later' following waters, all pumped samples are apparently enhanced in SO_4 contents over and above a simple freshwater–seawater mixing (Fig. 10). For the highest salinity samples (c. 9000 mg/L and greater) there appears to be a general trend to increasing SO_4 concentrations and SO_4/Cl ratios with decreasing chlorinity as the Frances waters are pumped over time, i.e. 'later' samples trend away in time from a simple seawater mixing line (Fig. 10). Since the Cl-concentrations can be modified only by evaporative concentration, mineral dissolution or mixing, enhanced SO_4/Cl ratios imply source(s) of SO_4 addition to the evolving waters. Dissolved Fe concentrations (Fe_{tot}) show the same general chlorinity trend following SO_4, suggesting pyrite oxidation and $FeSO_4$ dissolution as likely sources (Fig. 4c). The highest Fe_{tot} concentrations in Pump Test #2 (~590 mg/L = 10.6 mol/L) translate to a potential stoichiometric production (1:2) of SO_4 concentration of ~2000 mg/L for the oxidation of pyrite (FeS_2) on top of a seawater mixing component. This is in reasonable agreement with actual maximum concentrations observed of c. 4100 mg/L (after accounting for ~25–50% seawater mixing component with ~2700 mg/L SO_4).

A genetic cross-plot of the Frances waters from Pump Test #1 generally shows SO_4 isotopic signatures very different from seawater (Fig. 11). The $\delta^{18}O(SO_4)$ of ocean water is +9.5‰, with $\delta^{34}S(SO4)$ characteristically +21‰ (Krouse and

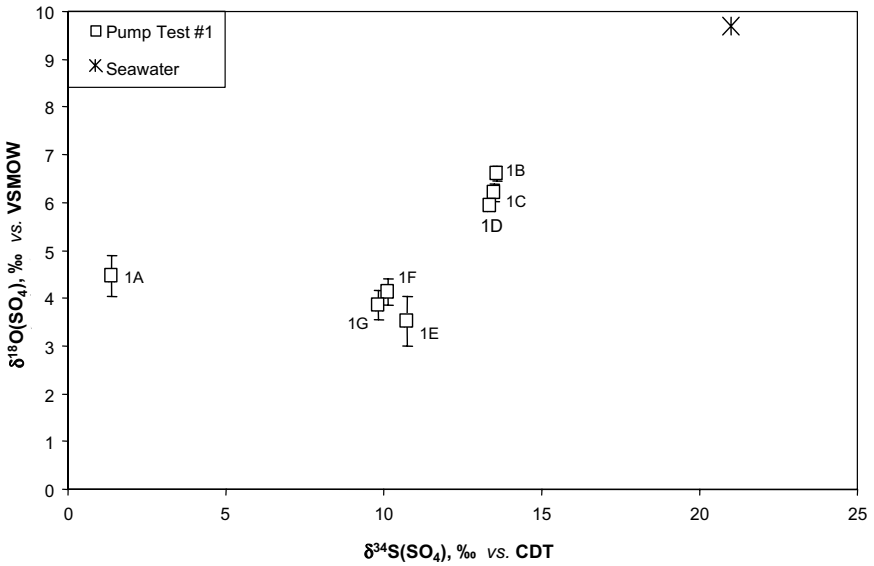

Fig. 11. Genetic cross-plot of stable isotope of SO_4($\delta^{18}O$, $\delta^{34}S$) signatures for the continuously-pumped water samples from the Frances mineshaft for Pump Test #1 (open squares), showing apparent evidence of $FeSO_4$ (melanterite) dissolution imprinted on a seawater mixing source especially for the later pumped waters. Two-component mixtures having different concentrations of SO_4 and also different isotopic ratios would be expected to lie on a linear mixing line when the concentration coordinates are transformed to [1/SO_4] on the *x*-axis (Faure, 1988, pp.142–144; Ingri et al., 1997). The characteristic signature for Seawater is also plotted. 'Early flush' waters are characterised as samples 1B–1D; 'later' waters are characterised as samples 1E–1G.

Mayer, 2000). The Frances pumped waters show $\delta^{18}O(SO_4)$ around +4 to +5‰, with $\delta^{34}S(SO_4)$ between +10 and +14‰. These values potentially plot at the more enriched ends of the signatures typically found for SO_4 derived from the oxidation of reduced inorganic sulfur compounds; evaporitic SO_4 sources typically would plot to even more isotopically heavier contents both in ^{34}S and ^{18}O (cf. Krouse and Mayer, 2000, their Fig. 7.3). The three most enriched $^{34}S(SO_4)$ and $^{18}O(SO_4)$ Frances sample signatures which reflect impact of the 'early flush' waters plot closest to a seawater signature, but generally all samples also show the influence of SO_4 generation over and above a characteristic seawater SO_4 isotopic signature. The 'later' waters show relatively lighter isotopic signatures that over time evolve further away from the seawater value as the dissolved SO_4 concentrations increase, and display signatures much more characteristic of SO_4 derived predominantly from oxidation of reduced inorganic sulfur compounds.

A cross-plot of the $\delta^{34}S(SO_4)$ vs. $1/[SO_4]$ (Fig. 12) suggests: (i) that lowest SO_4 samples apparently follow a freshwater mixing line with seawater, and; (ii) the higher SO_4 concentrations follow a linear trend of lightening $\delta^{34}S$ signature with increasing SO_4, which on extrapolation again intercepts a seawater mixing-line. This intercept suggests a SO_4-concen-

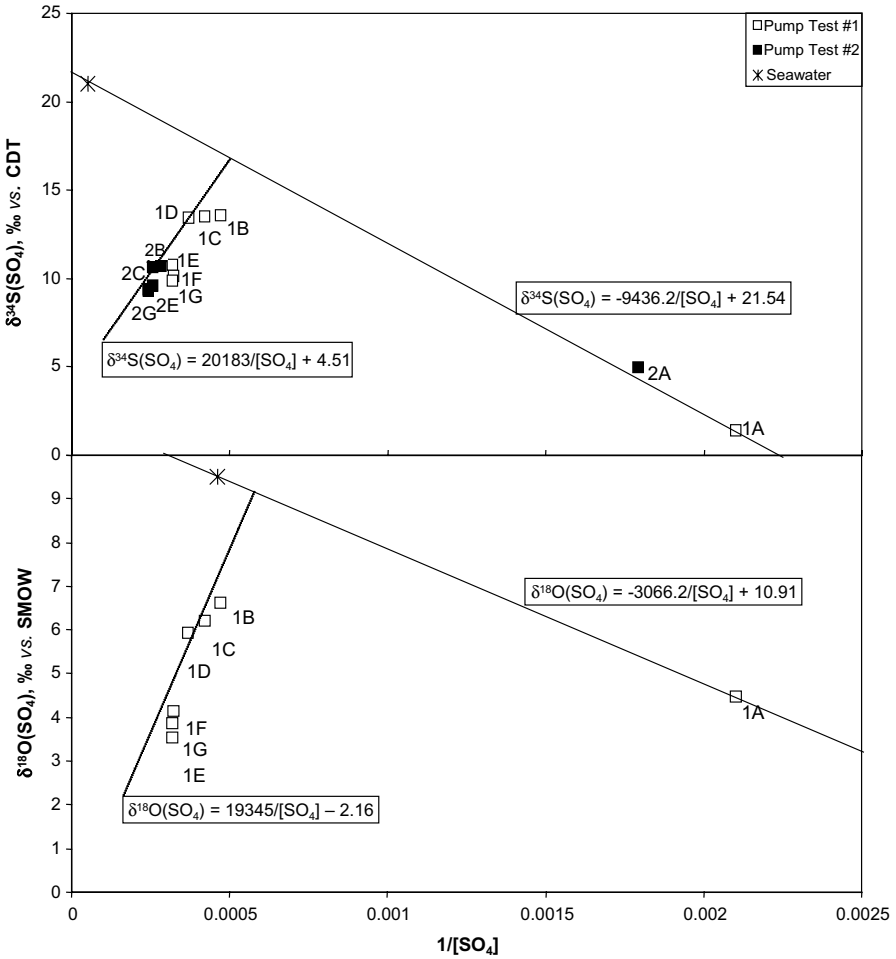

Fig. 12. Cross-plot of stable isotopes of SO_4 ($\delta^{18}O$, $\delta^{34}S$) signatures vs. $1/[SO_4]$ for the continuously-pumped water samples from the Frances mineshaft for Pump Test #1 (open squares), showing apparent evidence of two-component mixing between freshwaters with a $FeSO_4$ (melanterite) dissolution source (especially for the later pumped waters) and a seawater source. The characteristic signature for Seawater is also plotted. 'Early flush' waters are characterised as samples 1B–1D (Pump Test #1) and 2B–2C (Pump Test #2); 'later' waters are characterised as samples 1E–1G (Pump Test #1) and 2D–2G (Pump Test #2).

tration of c.1200 mg/L or 44% seawater mixing, in line with the $\delta^{18}O$ signature (Fig. 8) – although this does not take account of the enhanced SO_4-contents in the initial pumped waters due to any other sources (such as any component of water–rock interaction). A similar cross-plot for $\delta^{18}O(SO_4)$ vs. $1/[SO_4]$ (Fig. 12), suggests an intercept of only ca. 470 mg/L or 17% direct seawater mixing overall. Trend (ii) for the higher SO_4 waters particularly suggests a mono-source term (sulfide oxidation) end-member for the lighter S-isotopic signatures which increasingly predominates as SO_4 generation occurs and/or the products of sulfide oxidation dissolve in the 'later' pumped waters. The intercept of this second trend (ii) with the seawater-freshwater mixing line (trend (i)) also supports the notion that the component for the 'later' pumped waters leading to gradually reducing chlorinity over time (Figs 8 and 9) itself represents an admixed end-member or a dynamic balance between freshwater and seawater mixing of around equal proportions but involving now a significant source of SO_4 accumulation.

The apparent concomitant increase of SO_4 and Fe_{tot} in the Frances pumped minewaters (Figs 4a–4c) implicates the recovery of pumped minewaters increasingly affected by the results of pyrite oxidation and $FeSO_4$ dissolution. Oxygen isotope fractionation $[\Delta^{18}OSO_4–H_2O = \delta^{18}O(SO_4) - \delta\ ^{18}O(H_2O)]$ between dissolved SO_4 and water is generally characteristic of the potential oxidation processes for reduced S species (Taylor and Wheeler, 1994). For the Frances waters, the apparent 'raw' $\Delta^{18}OSO_4–H_2O$ (i.e. uncorrected for mixing effects) are between +7 and +12‰ (Table 6a; Krouse and Mayer, 2000), lying between the potential signatures for the O in the SO_4 being derived from either dissolved O_2 or the water (H_2O) itself (see below). The 'raw' values reflect a mixed signature of SO_4 derived from seawater component and SO_4 generated by sulfide oxidation; correction of the observed $\delta^{18}O(SO_4)$ signatures for the effects of a conservative mixing of SO_4 sources [Appendix A(ii)] then gives $\Delta^{18}OSO_4–H_2O$ between +9.5 (in the 'early flush' waters) and c. 0‰ (in the 'later' waters) (Fig. 13).

The oxidising agents for reduced S species in acid minewaters (Van Stempvoort and Krouse, 1994) generally are either dissolved (aq) molecular O_2 ($\delta^{18}O$ = c. +24‰) as a direct, primary source of oxidation:

$$S^{2-} + 2O_2 \rightarrow SO_4^{2-} \quad (1)$$

or through secondary sources such as the water molecule via oxidising agents other than O_2 (eg. Fe^{3+}), eg.:

$$S^{2-} + 8Fe^{3+} + 4H_2O \rightarrow SO_4^{2-} + 8Fe^{2+} + 8H^+ \quad (2)$$

Taylor and Wheeler (1994) suggest an equilibrium isotope enrichment factor, ε_{O2}, for a dissolved O_2 source of c. −8.7‰ in neutral to alkaline environments, or $\varepsilon_{O2} = -11.4$‰ in acid environments.

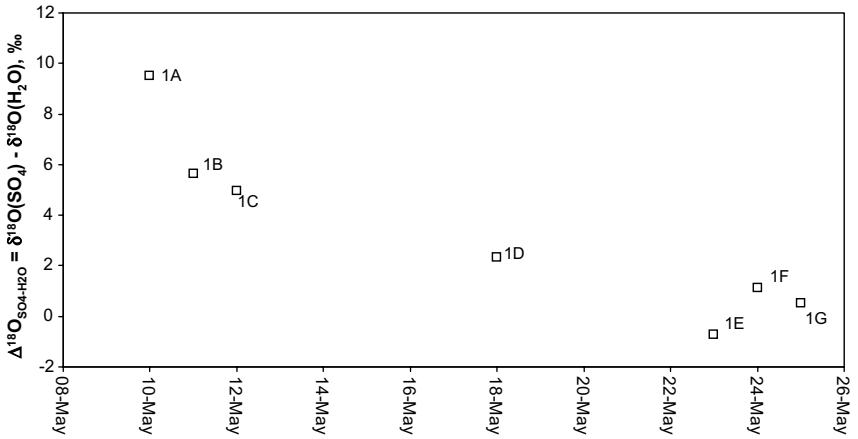

Fig. 13. Time evolution of $\Delta^{18}OSO_4–H_2O = \delta^{18}O\ (SO_4) - \delta^{18}O\ (H_2O)$ signatures for the continuously-pumped water samples from the Frances mineshaft for Pump Test #1 (open squares) after correction for possible mixing with a characteristic seawater source [see Appendix A(ii)], and showing apparent evidence of the change in predominance of the oxidising agent for the $FeSO_4$ (melanterite) dissolution as being due to predominantly primary oxidation by O_2 in early waters to a secondary source of oxidation for the (H_2O as the O-donating agent) in later waters. 'Early flush' waters are characterised as samples 1B–1D; 'later' waters are characterised as samples 1E–1G.

Hence the $\delta^{18}O(SO_4)$ for SO_4 deriving its O all from dissolved O_2 would give values around +13‰, closer to that seen in the lowest SO_4 content pumped waters associated with the 'early flush' in Pump Test #1. The fractionation factor for water is taken as $\varepsilon_{H_2O} = 0‰$, signatures therefore reflecting the genetic water source directly. The higher SO_4 waters with the isotopically lighter values pumped at Frances therefore suggest a mixed source but trending to a predominating source of O derived from local H_2O molecules and more ^{18}O-depleted values in the 'later' waters (Fig. 13). This implicates the imprinting effects of secondary weathering of source sulfides under predominantly aqueous conditions in these 'later' waters (cf. McCarthy et al., 1998).

Other explanations for the evolution of lighter S isotopic signatures in the 'later' pumped waters (Fig. 13) might invoke SO_4 reduction (and potential exchange of O-isotopes between the SO_4 and H_2O) or O-donors other than molecular O_2. However, there is little strong evidence for microbial SO_4 reduction in the Frances waters apart from the presumptive assertion by Nuttall et al. (2002a) that discharges at the wellhead "smelt strongly of H_2S"; moreover, SO_4 reduction fractionation characteristically for $\delta^{18}O(SO_4)$ should lead to evolution of isotopically heavier (and not lighter) values (Chiba and Sakai, 1985; McCarthy et al., 1998). So-called "denitrification-sulfate" (cf. Strebel et al., 1990; Aravena and Robertson, 1998) has an apparent fractionation factor of $\Delta^{18}OSO_4$–H_2O ~−8‰, similar to the fractionation effects for O isotope fractionation from a molecular (dissolved) O_2 source in neutral waters. This could give then isotopically lighter SO_4 isotopic signatures, but the potential for NO_3 reduction effects in the Frances waters is probably relatively small given the NO_3 content changes involved (Table 5). The S-isotopic signatures seen in the Frances waters are most likely due to admixture of a seawater source and (over and above this) sulfide oxidation and SO_4 generation both directly by (primary) molecular O_2 as seen in the 'early' phase of pumping and (secondary) the water itself as seen in the 'later' waters.

4.3. Residence time indicators

The initial ^3H activities ($\tau_{1/2} = 12.43$a) at start of pumping are likely sourced from a freshwater component, although a modern seawater contribution cannot be readily excluded. The low ^{14}C activity ($\tau_{1/2} = 5730$a) taken together with ^3H suggests either a mixed water signature in which young waters mix with an ancient water component (eg Mazor et al., 1986), or a young water system reflecting the effects of geochemical maturation in the C isotope systematics. The observed $\delta^{18}O(H_2O)$ signatures throughout the pump tests do not suggest the impact of any ancient palaeowater component related e.g. to the last Devensian glaciation (the most recent climate change, for which isotopic signatures of recharge waters would give relatively light $\delta^{18}O$, δ^2H signatures in the UK – cf. Elliot, 1999; Elliot et al., 1999). The initial bulk $\delta^{13}C(TDIC)$ value of −3.74‰ seen for example in Pump Test #1 already is relatively heavy with respect to typical recharge waters (cf. McNeill et al., 2003), which suggest the impact of water–rock interaction and dissolution of carbonate mineral phases with relatively high ^{13}C content.

The reduced ^3H activity in waters sampled after the first 24 h of recent water(s) is consistent with admixture with a component effectively devoid of ^3H (i.e. having a residence time >40a). During the 'early flush' waters the $\delta^{13}C$ (TDIC) signatures become isotopically lighter suggesting the influx of less evolved waters. The timing of the apparent initial increase also in specific ^{14}C activity of ca. 4–5 pmc seen in the Pump Test #1 data again suggests that these waters have been affected by the induced leakage ('early flush') waters recirculating from the lagoons which have exchanged $^{14}CO_2$ from the atmosphere, rather than being an artefact of possible CO_2 degassing (Nuttall et al., 2002a) and isotopic fractionation of samples (for which estimated pCO_2 values of all Frances samples remain enhanced over atmospheric, and does not point to degassing or open system conditions for which an equilibrium enrichment factor ε_{CO_2-HCO3} (14 °C) would be −9‰ for $\delta^{13}C$ and only −2% for ^{14}C; cf. Pearson et al., 1978; Mook, 1980). However, the concomitant decrease in ^3H values suggests also dynamic mixing of an older, evolved component for which ^3H is low or zero. The possibility that the lighter isotopic $\delta^{13}C$ signatures source from either the oxidation of reduced organic matter (cf. Thorstenson et al., 1979) and/or gases emanating from the coal measures themselves (giving oxidisable CH_4 with isotopically light $\delta^{13}C$ and δ^2H signatures) has not however been investigated. The comparatively oxidising Eh and relatively heavy stable isotope signatures observed in the pumped Frances waters suggest that this likely is not a pre-

dominant process. Subsequent and 'later' waters in Pump Test #2 then indicate an increasingly light $\delta^{13}C$ signature (Table 6b), and along with enhanced ^{3}H and ^{14}C activities these signatures suggest increasing admixing of younger, less evolved waters being drawn in over the longer term, possibly reflecting the ZOI capturing a younger end member component to mix with the modern waters after the 'early flush' behaviour or a shift in the dynamic balance of the contributing mixing end-member waters.

4.4. A hypothetical geochemical model

Nuttall and Younger (2004, their Fig.6)) have already postulated that the drastic water quality changes observed initially over the first 24 h of sampling reflect breakdown of water quality stratification in the Frances shaft. Geochemical modelling potentially can help further constrain/support the interpretation of sources and reaction pathways for the observed waters over the course of extended pumping. NETPATH (Plummer et al., 1994) has been used here, an inverse geochemical mass-balance model for calculating potential mixing proportions of given end-member waters along with subsequent plausible net geochemical pathways that can account for the observed final water. As the results of mass-balance modelling typically are non-unique (e.g. Tellam and Lloyd, 1986), NETPATH further allows forward modelling of selected isotopic signatures to constrain/select appropriate scenarios. The isotopes available for forward reaction modelling for the Frances pumped waters are ^{13}C, ^{14}C and ^{34}S. Since these are generally available only for the Pump Test #1 data, only the scenarios relating to this test are discussed. Based on the previous discussion above potential sources and pathways of reaction include:

- Mixing of waters (fresh, sea, recirculating surface lagoon waters) [affecting Cl, Br and influencing $\delta^{18}O(H_2O)$ signatures].
- Dissolution of mineral carbonates affecting carbon systematics and/or potential source/loss of CO_2 (open vs. closed system) [influencing $\delta^{13}C$, ^{14}C signatures].
- Dissolution of melanterite [affecting Fe and SO_4 concentrations and influencing $\delta^{34}S$ signatures].

Elemental constraints modelled are: C, Ca, Mg, Fe, Mn, S, Al. Mineral phase constraints [as source/sink for particular elements] include calcite [Ca, C], dolomite [Ca, Mg, C], rhodochrosite [Mn, C], CO_2 gas [C], goethite [Fe], gibbsite [Al], + melanterite [Fe, S], siderite [Fe, C]. Only melanterite is forced as a dissolving phase (+) in all scenarios. Oxygen-18 is also included as an element and used to constrain mixing ratios (similar results are given when using ^{3}H data). For the forward modelling the carbonate minerals were assigned $\delta^{13}C = 0‰$, $^{14}C = 0$ pmc. Melanterite dissolution was assigned a reasonable value for the $SO_4\delta^{34}S$ of $-10‰$ (Krouse and Mayer, 2000). For open system scenarios only a CO_2 gas phase was included in the model with designated values of $\delta^{13}C = -25‰$, $^{14}C = 100$ pmc.

The initial freshwater used was Kinnesswood No.2 from McNeill et al. (2003). This fresh, shallow groundwater in the Upper Devonian Sandstone Aquifer in Fife has a measured ^{3}H activity of ~12 TU and $\delta^{18}O = -8.9‰$. In NETPATH modelling it is assigned $^{14}C = 85$ pmc as a recharge water. The seawater hydrochemistry is taken from Drever (1997), but assigned the following isotopic signatures assuming a modern seawater composition (Craig, 1961; Mook, 1980; Krouse and Mayer, 2000): $\delta^{18}O = 0‰$, $\delta^{2}H = 0‰$, $\delta^{13}C = -2‰$, $^{14}C = 80$ pmc, $\delta^{34}S(SO_4) = +21‰$. Since the end member signatures for mixing/reaction are for the most part hypothetical and used simply to qualitatively illustrate plausible models, in model scenarios agreement was taken to be when forward modelling from mass-balance calculations had reproduced the observed $\delta^{13}C$ (TDIC) and $\delta^{34}S(SO_4)$ within ± few ‰ and also ^{14}C within ± few %.

For Pump Test #1 data (Tables 5, 6a and 6b), preliminary modelling initially assumed only a two-component mixing between initial fresh- and sea-water with subsequent reaction to the final water. Forward modelling results could approach the $\delta^{34}S(SO_4)$ signatures observed – confirming melanterite dissolution on top of seawater mixing as a plausible reaction pathway. However, this scenario could not reproduce the observed $\delta^{13}C$(TDIC) and ^{14}C signatures, invoking therefore another source of radiocarbon input. The signatures could be reproduced only when a third component of admixing initial water was introduced. The hydrochemical evidence points to an 'early flush' phenomenon and recirculating waters associated with leakage of the surface lagoons. In this latter NETPATH modelling scenario for the recirculating waters component the most recent mine-water sample in the sequence having a full chemical and isotopic composition (Table 5) was

mixed in, reflecting the possible influence of surface lagoon waters. However, since these are now recirculating surface waters admixing, the initial ^{14}C activity for these components were adjusted to have ^{14}C activity of their TDIC as 100 pmc reflecting potential exchange and equilibration of $^{14}CO_2$ activity from the atmosphere prior to their infiltration and mixing in the subsurface. This scenario of three-component mixing then qualitatively reproduced the observed ^{13}C, ^{14}C, and ^{34}S of the Pump Test #1 mine waters, giving the following simulated mixing ratios:

(i) For 11 May sample (using 10 May water as the recirculation water adjusted to have $^{14}C_{TDIC} = 100$ pmc):
Fresh water = 39%
Sea water = 60%
Recirculation (lagoon) water = 1%
i.e. in line with seawater mixing estimates of Younger et al. (1995).

(ii) For 18 May sample (using 11 May water as the recirculation water adjusted to have $^{14}C_{TDIC} = 100$ pmc):
Fresh water = 3%
Sea water = 15%
Recirculation (lagoon) water = 82%

(iii) For 24 May sample (using 23 May water as the recirculation water adjusted to have $^{14}C_{TDIC} = 100$pmc):
Fresh water = 18%
Sea water = 21%
Recirculation (lagoon) water = 60%

The hypothetical model therefore invokes three-component mixing for the Frances waters and supports the notion that whilst mixing of fresh waters and seawater indeed is implicated, recirculating waters predominate the Pump Test #1 data (see (ii) above), although their impact lessens towards the end of the Pump Test. ^{14}C activity is brought in to the system through the TDIC of the recirculating waters component of mixing. Over and above the freshwater–seawater mixing, dissolved SO_4 chemical and isotopic signatures are supported by further sulfide oxidation reaction here represented by melanterite ($FeSO_4$) dissolution. Inverse modelling suggests that a free CO_2 gas phase (reflecting open system conditions and direct exchange with the atmosphere) is not required in the NETPATH simulations, i.e. the simulated geochemical reactions occur essentially under closed system conditions following the mixing and reaction of initial waters to give the final water condition.

Note particularly for simulation (i) that water quality changes over the first 24 h or so of Pump Test #1 do not require the input of recirculation waters but reflect instead simply a possible freshwater–seawater mixing (i.e. potentially destratification of the shaft waters) upon which a degree of $FeSO_4$ dissolution is imprinted. The enriched $\delta^{34}S(SO_4)$ and $\delta^{18}O(SO_4)$ values relative to 'later' waters support this seawater mixing influence. The NETPATH mass balance modelling also then supports the freshwater–seawater mixing calculations presumed originally by Nuttall and Younger (2004) for the turbulent breakdown of the initially stratified column.

Unfortunately, for Pump Test #2 data only one sample was submitted for ^{14}C(TDIC) analysis and none for $^{34}S(SO_4)$. Nevertheless, as the Pump Test #2 data shows a similar 'sag' phenomenon presumed related to lagoon water recirculation it is likely that a similar conceptual model to the above applies in that case.

4.5. A post-script to the initial pumping tests results

Most recently, Johnson et al. (2004) have updated the Frances study since the completion of initial stepped pumping tests in 2000. A second phase of test pumping at Frances began in Spring 2003. However, this time poor water quality did not in fact emerge at the wellhead in this test pumping. Johnson et al. (2004) suggest that because the water level at Frances was below the level of Randolph (invoked as the source of poor quality waters) flow was preferentially towards Frances during the 2000 tests. In 2003, by contrast, following substantial further rainfall recharge to the system over the intervening $2\frac{1}{2}$-years period between the two Pump Test programmes (when the shaft was not therefore being actively pumped), water levels in the Frances shaft had become similar if not higher than the Randolph Pond (for which a static water level of c. −32.4 m AOD has prevailed). This further water storage in the Frances system then masks the underlying poor water quality threat seen in the earlier tests.

4.6. Is Randolph Pond directly a predominating component of mixing to the Frances shaft?

During active operation pumped Frances waters typically displayed only circum-neutral pH and Fe

values an order of magnitude less than seen in the Frances pumped waters following mine water rebound. Nuttall et al. (2002b) postulated therefore that only the consistently low pH and high Fe-loading seen historically in Randolph Pond waters matches the chemistry achieved during the recent pumping tests at Frances. Since the Dysart Main seam provides connection between Frances and Randolph, Nuttall et al. (2002b) speculated therefore that Randolph Pond sources a component of the poor quality water seen in the Frances shaft. Alongside the water table recovery behaviour of the Randolph Pond identified by Johnson et al. (2004), this implies an active drawing in of waters from the Randolph Pond as potentially a significant source of poor water quality. On a $\delta^{18}O$–Cl plot (Fig. 8) the pumping Frances waters with diluting chlorinity apparently trend towards the single Randolph sample signature (Table 5, Table 6a) taken during the recent Pump Test #1, suggesting that the Randolph Pond may be involved as a component of the 'later' diluting waters. However, this Randolph sample is likely enriched in $\delta^{18}O$ as an artefact of sampling. Samples taken from the Randolph Pond in 1971 and more recently (Younger et al., 1995) record in fact a more alkaline water signature developed rather than the acidic waters seen historically. The single Randolph sample taken during Pump Test #1 shows a Br-concentration effectively below detection and a F-content of c. 2.8 mg/L, whereas all of the pumped Frances waters are essentially devoid of dissolved F (excepting a singular sample at the start of Pump Test #2 with c. 0.3 mg/L F, close to the limit of detection). Moreover, the SO_4/Cl ratio of the Randolph sample is also significantly different from the 'later' pumped waters at Frances (Fig. 10). Thus, whilst better characterisation of the waters in the Randolph Pond would be needed to explore any potential contribution further, current evidence suggests that the poor quality waters (high metals loadings, high SO_4) in the later pumped waters at Frances reflect simply the 'pull-back' of rebound waters in Frances which had come into contact with higher S-content parts of the Main Dysart seam through the worked connections rather than necessarily an active drawing in of waters from Randolph Pond.

5. Conclusions

Nuttall and Younger (2004) have previously discussed the breakdown of water quality within the first 24 h of active pumping of a static, stratified, rebound water table in the Frances mineshaft during the first test pumping phase (2000) following abandonment of operational pumping 5 years previous. Initially there was a mixing of bottom and top water qualities induced by turbulent flow in the shaft on active pumping even at a relatively shallow depth in the water column. A range of hydrochemical and isotopic parameters have been analysed on recovered samples following the extended pumping over several weeks, to identify further the water sources, mixing dynamics, and hydrogeochemical evolution of the pumped Frances system.

Mixing indicators ($\delta^{18}O$, Br/Cl) clearly identify seawater as a component source of salinity in all of the pumped Frances waters. The initial Frances waters apparently display a seawater mixing with a freshwater component of $\delta^{18}O$ $\sim 7‰$. Nuttall and Younger (2004) have commented that evidence for a seawater salinity source is interesting for the Frances mine in that its undersea portions were always dry and repeated safety assessments never found evidence for any seawater ingress during operational pumping. Johnson et al. (2004) suggest that the seawater component may reflect ingress routed through connection at the base of the Frances shaft with the adjacent coastal Michael workings.

Apart from intrusion of a seawater component, a second source of salinity is implicated from an evaporitic mineral source (giving e.g. a characteristic Br/Cl ratio ~ 0.002). This latter source is invoked to explain the salinity evolution in 'early flush' samples immediately following breakdown of water quality stratification in the shaft at the start of pumping and the ensuing expanding ZOI of the pumping. These 'early flush' waters are identified hydraulically with induced leakage from surface treatment lagoons and recirculation of these shallow waters to the shaft. The evaporitic source is likely rock salt used to de-ice the colliery yard during winter. The induced recirculation waters having contacted the mine spoil material lining the lagoons apparently produce a characteristic redox indicator 'sag' affecting the pumped water quality (cf. Søgaard et al., 2001). The impact of these waters is clearly evidenced during Pump Test #1 and to a lesser extent at the start of Pump Test #2 before the lagoons were lined. For Pump Test #2, the leakage does not influence the subsequent hydraulic step-drawdown results after lining the lagoons but still impacts the pumped water quality. Subsequent to the impact

of recirculation waters, either because of a degree of self-sealing of the lagoons (Pump Test #1) or because proper lining of the lagoons had been completed (Pump Test #2), the water quality impacts of the 'early flush' phenomenon are diluted away slowly over time in 'later' waters as subsequent pumping draws in fresh and seawater components apparently in more or less in equal proportions.

Whilst the initial waters (including the recirculating 'early flush' waters) in both tests show predominantly a freshwater–seawater mixed signature, increasing dissolved SO_4 concentrations are clearly evidenced for the 'later' waters over and above a freshwater–seawater mixing line (identified also by S-isotopic systematics) and associated with enhanced dissolved Fe-loading. Sulfur isotopic signatures identify the influence of the products of sulfide oxidation in the pumped waters initially with a strong signature of primary oxidation by molecular O_2 ($\delta^{18}O(SO_4) = c.\ +13‰$) associated apparently with the recirculation waters which have contacted mine spoil material, but subsequently showing also secondary oxidation of source sulfides by the water molecule itself and SO_4 generation in the 'later' pumped waters.

Overall, hypothetical mass balance (NETPATH) modelling of the hydrogeochemical evolution of the pumped minewaters identifies generally a three-component mixing involving freshwater, seawater and the impact of recirculation (lagoon) waters. Estimates of the extent of freshwater–seawater mixing range from 40 to 60% at the start of the pumping tests, to ~20–50% in the later waters in line with the hypothetical modelling. The effect of the lagoon water recirculation postulated by Nuttall et al. (2002a) on the basis of hydraulic measurements alone then is seen to be significant, initially predominating the water quality directly after the breakdown of stratification in the shaft. The observed C- and S-isotopic signatures can be modelled by additional carbonate mineral and melanterite ($FeSO_4$, as the product of pyrite oxidation) dissolution.

Although Nuttall et al. (2002a) have suggested that poor water quality in these pumped waters reflects mixing-in of highly acidic, highly ferruginous waters potentially actively drawn in from the Randolph mine, an alternative interpretation favoured by e.g. the S-isotope systematics suggests instead that the diluting component for the more saline waters is in fact a mix of fresh and seawater components affected now by pyrite oxidation/$FeSO_4$ dissolution in the Frances system. The poor water quality seen in the first phase (2000) of pumping tests probably relates to Frances waters coming in contact with the higher sulfur content (S%) Dysart Main seam such as seen towards Randolph or another high-S seam with significant acid-generating potential.

Finally, the fact that further test-pumping of the Frances shaft in 2003 after a further $2\frac{1}{2}$-years period of water recovery in the system did not again encounter poor quality waters, put alongside the original seawater ingress likely from the connection of Frances to Michael Colliery, again strongly asserts the role of hydrodynamics of connected mineworking voids generally in controlling both flows and water qualities. If this better quality recharge storage is removed from the Frances system then the poor quality water may well reappear.

Acknowledgements

Thanks go to: Dr. Charlotte Nuttall (University of Newcastle) for collecting water samples and providing IC and ICP-MS (cation) results; Angela Downey (sample precipitations for ^{14}C and S-isotopes; $\delta^{18}O$, $\delta^{2}H$ of water analyses, 'specific' $\delta^{13}C$ and HS^- analyses), Dr. Neil Ogle (CO_2 gas preparation for ^{14}C analyses and 'bulk' $\delta^{13}C$ analyses) and Mike Matiasek (IC anions) of the QUB EERC; John Morrison (Micromass, UK) for SO_4 isotopic ($\delta^{18}O$, $\delta^{34}S$) analyses; Dr. Christopher J. Eastoe for ^{3}H analyses (Laboratory of Isotope Geosciences, University of Arizona, USA; see http://www.geo.arizona.edu/researchers/mbaker/AustinLong/); and Dr. A.J. Timothy Jull for ^{14}C analyses (NSF Accelerator Mass Spectrometry Group, University of Arizona, USA; see http://www.physics.arizona.edu/ams/). This work was funded from an Urgency Grant (GR3/13205) from the Natural Environment Research Council (NERC).

Appendix A

(i) Calculating fraction (f) of mixing from $\delta^{18}O(H_2O)$:

$$\delta^{18}O_{sample} = f.\delta^{18}O_{seawater} + (1-f).\delta^{18}O_{freshwater} \quad (A.1)$$

$$(1-f) = \delta^{18}O_{sample}/\delta^{18}O_{freshwater} \quad (A.2)$$

Taking $\delta^{18}O_{seawater} = 0‰$; $\delta^{18}O_{freshwater} = -8.9‰$ (cf. Kinnesswood No. 2, McNeill et al., 2003) then

$$f = 1 - [\delta^{18}O_{sample}/(-8.9)] \quad (A.3)$$

(ii) Correcting $\delta^{18}O(SO_4)$ signatures of reaction for conservative mixing effects:
By mass balance for SO_4 concentration components:

$$[\delta^{18}O.SO_4]_{sample} = [\delta^{18}O.SO_4]_{freshwater} + [\delta^{18}O.SO_4]_{seawater} + [\delta^{18}O.SO_4]_{add} \quad (A.4)$$

where 'add' represents SO_4 input from reaction source(s). Assuming the concentration of $SO_{4,freshwater}$ is negligible in comparison to the other components,

$$[\delta^{18}O.SO_4]_{sample} \approx [\delta^{18}O.SO_4]_{seawater} + [\delta^{18}O.SO_4]_{add} \quad (A.5)$$

From (i) above and taking f (fraction of seawater mixing in sample) as defined by Eq. A.3, then

$$SO_{4,seawater} = f.SO_{4,sample} \quad (A.6)$$

$$SO_{4,add} = (1-f).SO_{4,sample} \quad (A.7)$$

Hence,

$$\delta^{18}O_{sample}.SO_{4,sample} \approx \delta^{18}O_{seawater}.f.SO_{4,sample} + \delta^{18}O_{add}.(1-f).SO_{4,sample} \quad (A.8)$$

and

$$\delta^{18}O_{add} \approx [\delta^{18}O_{sample}.SO_{4,sample} - \delta^{18}O_{seawater}.f.\ SO_{4,sample}] /(1-f).SO_{4,sample} = [\delta^{18}O_{sample} - f.\delta^{18}O_{seawater}]/(1-f) \quad (A.9)$$

Taking $\delta^{18}O$ seawater $= +9.5‰$

$$\delta^{18}O_{add} \approx [\delta^{18}O_{sample} - f.(+9.5)]/(1-f) \quad (A.10)$$

Thence, use Eq. (A.10) and $\Delta^{18}OSO_4{-}H_2O = \delta^{18}O(SO_4) - \delta\ ^{18}O(H_2O)$ to estimate the O isotope fractionation of reaction.

References

Aravena, R., Robertson, W.D., 1998. Use of multiple isotope tracers to evaluate denitrification in ground water: Study of nitrate from a large-flux septic system plume. Ground Water 26, 975–982.

Ball, J.W., Nordstrom, D.K., 1991. User's Manual for WATEQ4F, with Revised Thermodynamic Data Base and Test Cases for Calculating Speciation of Trace, Major and Redox Elements in Natural Waters. US Geol. Surv. Open Rep., 91–183.

Carmody, R.W., Plummer, L.N., Busenberg, E., Coplen, T.B., 1998. Methods for the collection of dissolved sulfate and sulfide and analysis of their sulfur isotopic composition. US Geol. Surv. Open Rep., 97–234.

Chiba, H., Sakai, H., 1985. Oxygen isotope exchange-rate between dissolved sulfate and water at hydrothermal temperatures. Geochim. Cosmochim. Acta 49, 993–1000.

Clarke, W.A., Konhauser, K.O., Thomas, J.C., Bottrell, S.H., 1997. Ferric hydroxide and ferric hydroxysulfate precipitation by bacteria in an acid mine drainage lagoon. FEMS Microbiol. Rev. 20, 351–361.

Craig, H., 1961. Isotopic variations in meteoric waters. Science 133, 1702–1703.

Douglas, S., Beveridge, T.J., 1998. Mineral formation by bacteria in natural microbial communities. FEMS Microbiol. Ecol. 26, 79–88.

Drever, J.I., 1997. The Geochemistry of Natural Waters. third ed. Prentice Hall, USA.

Edmunds, W.M., 1975. Geochemistry of brines in the coal measures of northeast England. Trans. Inst. Min. Metal. (Section B) 84, 39–52.

Elliot, T., 1999. Palaeo-ages of groundwaters in a fissured Chalk aquifer, UK. In: Isotope Techniques in Water Resources Development and Management, Proc. IAEA Internat. Symp. 10–14 May 1999, Vienna, Austria. Section 4, IAEA SM-361/31, pp. 144–155.

Elliot, T., Andrews, J.N., Edmunds, W.M., 1999. Hydrochemical trends, palaeorecharge and age of groundwaters in the fissured Chalk of the Berkshire and London Basins. UK Appl. Geochem. 14, 333–363.

Faure, G., 1988. Principles of Isotope Geology. second ed. John Wiley, New York, USA.

Gasharova, B., Göttlicher, J., Becker, U., 2005. Dissolution at the surface of jarosite: an in situ AFM study. Chem. Geol. 215, 499–516.

Grenthe, I., Stumm, W., Laaksuharju, M., Nilsson, Wikberg, P., 1992. Redox potentials and redox reactions in deep groundwater systems. Chem. Geol. 98, 131–150.

Hoth, N., Feldmann, H., Rinker, A., Glombitza, F., Häfner, F., 2005. Reductive processes within lignite dumps – chance of a long-term natural attenuation process. Geoderma 129, 19–31.

Hounslow, A.H., 1995. Water Quality Data. CRC Press/Lewis Publishers, USA.

Ingri, J., Torssander, P., Abdersson, P.S., Mörth, C.-M., Kusakabe, M., 1997. Hydrogeochemistry of sulfur isotopes in the Kalix River catchment, northern Sweden. Appl. Geochem. 12, 483–496.

Johnson, K.L., Nuttall, C.A., Younger, P.L., 2004. Developing a predictive understanding of hydrological and hydrochemical changes in abandoned coalfields. Final Report for the Coal Authority, Hydrogeochemical Engineering Research and Outreach (HERO), University of Newcastle Upon Tyne, UK, December 2004.

Kalin, R.M., 2000. Radiocarbon dating of groundwater systems. In: Cook, P.G., Herczeg, A.L. (Eds.), Environmental Tracers in Subsurface Hydrology. Springer. Kluwer Academic, pp. 111–144 (Chapter 4).

Kendelewicz, T., Doyle, C.S., Bostick, B.C., Brown, G.E., 2004. Initial oxidation of fractured surfaces of $FeS_2(100)$ by molecular oxygen, water vapour, and air. Surf. Sci. 558, 80–88.

Knox, J., 1954. The Economic geology of the Fife Coalfields: Area III. Markinch, Dysart and Leven. Memoirs of the Geological Survey, Scotland, HMSO, Edinburgh.

Krouse, H.R., Mayer, B., 2000. Sulphur and oxygen isotopes in sulphate. In: Cook, P.G., Herczeg, A.L. (Eds.), Environmental Tracers in Subsurface Hydrology. Kluwer Academic, pp. 195–231 (Chapter 7).

Lloyd, J.W., Heathcote, J.A., 1985. Natural Inorganic Hydrochemistry in Relation to Groundwater: An Introduction. Oxford University Press, UK.

Macalady, D.L., Langmuir, D., Grundl, T., Elzerman, A., 1990. Use of model-generated Fe^{3+} activities to compute Eh and ferric oxyhydroxide solubilities in aerobic systems. In: Melchior, D.C., Bassett, R.L. (Eds.), Chemical Modeling of Aqueous Systems, II, Am. Chem. Soc. (ACS) Symp. Ser., 419, pp. 350–368.

Mazor, E., Jaffé, F.C., Fluck, J., Dubois, J.D., 1986. Tritium corrected ^{14}C and atmospheric noble gas corrected ^{4}He applied to deduce ages of mixed groundwaters: examples from the Baden region, Switzerland. Geochim. Cosmochim. Acta 508, 1611–1618.

McCarthy, M.D.B., Newton, S.H., Bottrell, S.H., 1998. Oxygen isotopic compositions of sulphate from coals: implications for primary sulphate sources and secondary weathering processes. Fuel 77, 677–682.

McNeill, G.W., Anderson, J., Elliot, T., 2003. Nitrate levels and the age of groundwater from the upper Devonian Sandstone aquifer in Fife, Scotland. Environ. Geochem. Health 25, 105–113.

Mook, W.G., 1980. Carbon-14 in hydrogeological studies. In: Fritz, P., Fontes, J-Ch. (Eds.), Handbook of Environmental Isotope Greochemistry The Terrestrial Environment, vol. 1.. A Elsevier, Amsterdam, pp. 9–74 (Chapter 2).

Munk, L., Faure, G., Koski, R., 2006. Geochemical evolution of solutions derived from experimental weathering of sulfide-bearing rocks. Appl. Geochem. 21, 1113–1123.

Nordstrom, D.K., 2000. Aqueous redox chemistry and the behaviour of iron in acid mine waters. In: Wilkin, R.T., Ludwig, R.D., Ford, R.G. (Eds) Proc. Workshop Monitoring Oxidation–Reduction-Processes for Ground-Water Restoration, Dallas, Texas, 24–27 April 2000, US Environmental Protection Agency, Cincinatti Ohio, USA, EPA/600/R-02/002, pp. 43–47.

Nordstrom, D.K., Jenne, E., Ball, J., 1979. Redox equilibria of iron in acid mine waters. In: Jenne, E.A. (Ed.), Chemical Modelling in Aqueous Systems, Am. Chem. Soc. (ACS) Symp. Ser., 93, pp. 51–79.

Nuttall, C.A., Younger, P.L., 2004. Hydrochemical stratification in flooded underground mines: an overlooked pitfall. J. Contam. Hydrol. 69, 101–114.

Nuttall, C.A., Adams, R., Younger P.L., 2002a. Frances and Deerplay Colliery Report, University of Newcastle upon Tyne.

Nuttall, C.A., Adams, R., Younger P.L., 2002b. Integrated hydraulic-hydrogeochemical assessment of flooded deep mine voids by test pumping at Deerplay (Lancashire) and Frances (Fife) Collieries. In: Younger, P.L., Robins, N.S. (Eds.), Mine Water Hydrogeology and Geochemistry, Geol. Soc. Lond., Spec. Publ. 198, pp. 315–326.

Pearson, F.J., Fisher, D.W., Plummer, L.N., 1978. Correction of groundwater chemistry and carbon isotopic composition for effects of CO_2 outgassing. Geochim. Cosmochim. Acta 42, 1799–1807.

Plummer, L.N., Prestemon, E.C., Parkhurst, D., 1994. An interactive code (NETPATH) for modeling NET geochemical reactions along a flow PATH – Version 2.0.. US Geol. Surv. Water Resour. Invest. Rep., 94–4169.

Richter, B.C., Kreitler, C.W., 1993. Geochemical Techniques for Identifying Sources of Ground-Water Salinization. C.K. Smoley/CRC Press Inc., Boca Raton, Florida, USA.

Sherwood, J.M., 1997. Modelling minewater flow and quality changes after coalfield closure. Unpublished Ph.D Thesis, Department of Civil Engineering, University of Newcastle upon Tyne, UK.

Smith, C.L., 1991. Proposed method of hydrogeochemical exploration for salt deposits using Cl–Br ratios, Eastern Province, Kingdom of Saudi Arabia. Appl. Geochem. 6, 249–255.

Søgaard, M., Larsen, F., Postma, D., 2001. Pyrite oxidation in unsaturated aquifer sediments Reaction stoichiometry and rate of oxidation. Environ. Sci. Technol. 35, 4074–4079.

Strebel, O., Böttcher, J., Fritz, P., 1990. Use of isotope fractionation of sulfate-sulfur and sulfate–oxygen to assess bacterial desulfurication in a sandy aquifer. J. Hydrol. 121, 155–172.

Taylor, B.E., Wheeler, M.C., 1994. Sulfur- and oxygen- isotope geochemistry of acid mine drainage in the Western United States: field and experimental studies revisited. In: Alpers, C.N., Blowes, D.W. (Eds), Environmental Geochemistry of Sulfide Oxidation. American Chemical Society (ACS) Symp. Series 550, pp. 481–514.

Tellam, J.H., Lloyd, J.W., 1986. Problems in the recognition of seawater intrusion by chemical means: an example of apparent chemical equivalence. Quart. J. Engin. Geol. 19, 389–398.

Thorstenson, D.C., Fisher, D.W., Croft, M.G., 1979. The geochemistry of the fox hills-basal hell creek aquifer in southwestern North Dakota and northwestern South Dakota. Water Resour. Res. 15, 1479–1498.

Van Stempvoort, D.R., Krouse, H.R., 1994. Controls of $d^{18}O$ in sulfate. In: Alpers, C.N., Blowes, D.W. (Eds), Environmental Geochemistry of Sulfide Oxidation. American Chemical Society (ACS) Symp. Series 550, pp. 446–480 (Chapter 29).

Wright, W.G., Nordstrom, D.K., 1999. Oxygen isotopes of dissolved sulfate as a tool to distinguish natural and mining-related dissolved constituents: In: Tailings and Mine Waste'99: A.A. Balkema, Netherlands, 671–678. Available on the USGS Abandoned Mine Lands Initiative (AMLI) website at http://amli.usgs.gov/amli/reports/wright_isotopes.pdf.

Younger, P.L., 1994. Frances and Michael Collieries Study: Report on the Effect of Ceasing Pumping from the Frances and Michael Collieries (94G168/001). Bullen Consultants for Forth River Purification Board, Scotland.

Younger, P.L., 2001. Mine water pollution in Scotland: nature, extent and preventative strategies. Sci. Total Environ. 265, 309–326.

Younger, P.L., Barbour, M.H., Sherwood, J.M., 1995. Predicting the consequences of ceasing pumping from the Frances and Michael Collieries, Fife. In: Black, A.R., Johnson, R.C. (Eds.), 5th National Hydrology Symposium, Heriot-Watt University, Edinburgh, Scotland, 4–7th September 1995, British Hydrological Society, pp. 2.25–2.32.